EUROPEAN JOURNAL OF MATERIALS SCIENCE AND ENGINEERING
Volume 7, Issue 4, 2022: 225-260 | www.ejmse.ro | ISSN: 2537-4338

DOI: 10.36868/ejmse.2022.07.04.225

METAL OXIDE ELECTRON TRANSPORT MATERIALS IN PEROVSKITE SOLAR CELLS: A REVIEW

Ankit Stephen THOMAS[1*]

[1]Department of Chemical Engineering, National Institute of Technology Karnataka, India

Abstract

The domain of third-generation photovoltaics, mainly perovskite solar cells (PSCs), has been a topic of intensive research due to its varied and renowned efficiency values. However, the concern of stability and long-term operational abilities is a subject that needs to be looked into very differently. Thus, Metal Oxide Electron Transport Materials (MO ETMs) evolved. This review explains the employment of MO ETMs in various PSC architectures, the different deposition methods, requirements of an ideal MO ETM, the common materials that have been used previously, strategies to improve MO ETM-based device performance and lastly, techniques to find and synthesize an appropriate MO ETM. The entire review depicts how one can find alternative approaches to the traditional methods/materials used in a PSC. Moreover, it also highlights the various barriers to commercialization and how one can overcome them using varied approaches like molecular engineering, bilayer techniques and so on, to produce efficient and stable devices.

Keywords*: perovskite solar cells; metal oxide electron transport materials; third-generation photovoltaics; device improvement strategies; solar cells.*

Introduction

A perovskite solar cell (PSC) is a third-generation photovoltaic device for its cheap materials and easy fabrication processes. A PSC has a few distinct components: perovskite active layer, charge transporting materials and electrodes.

The working principle of a PSC can be elaborated as follows: the incident radiation on the perovskite active layer generates electron and hole charge carriers. The respective charge transport materials then separate these charge carriers. Lastly, they can power an external load on coming in contact with the electrodes.

In the PSC domain, five research areas are being heavily researched to produce high-efficiency PSCs. The areas are namely, a) perovskite molecules and films, b) engineering methods for device optimization, c) improved charge transport materials and interfaces, d) optimal device architectures, and e) encapsulation and stability properties [1].

Typically, the materials used in a conventional electron transport material (ETM) are TiO_2, PEDOT:PSS and fullerenes. However, it is essential to understand that the function of an ETM is of utmost importance. It needs to not only efficiently transport electrons but block holes simultaneously. Along with being an efficient transport and blocking material, an ETM needs to have a suitable energy band alignment with the perovskite layer to facilitate a smooth transfer of charge carriers.

Organic and Inorganic materials are used in PSCs, which can work exceptionally well as ETMs. Organic ETMs are solution processible and flexible but suffer from high costs and poor

*Corresponding author: ankitsthomas@gmail.com

stability properties. Inorganic ETMs are low-cost, low-temperature, versatile and stable, giving these materials a slight edge over the former [2].

Metal Oxide electron transport materials (MO ETMs) are a separate class of materials. They are noted for their improved performance in devices, superior chemical and physical stability, and solvent compatibility is ideal for producing efficient and appropriate devices. Moreover, they have improved conductivity levels, reactive electronic transition, electrochromic properties and high dielectric constant. These are why MOs are actively used in optical devices like PSCs, fuel cells, photocatalysts and piezoelectric devices [3]. TiO_2 and SnO_2 are popular MO ETMs, and devices fabricated using these materials have produced excellent photovoltaic parameters. Wide bandgap MOs are the ones of current interest and are being extensively researched. The wide bandgap is necessary so that it does not absorb any light in the visible region. Wide bandgap MOs can be used as ETMs or hole-transporting materials (HTMs). In some cases, researchers have also found wide bandgap MOs as an interlayer to improve device performance and stability.

Delving deeper into the case of TiO_2, it is an active photocatalyst which directly impacts the stability of the perovskite layer and promotes its degradation. In the case of SnO_2, it has many dangling bonds which behave as trap sites to increase charge recombination. Moreover, these bonds also react with the atmosphere in ambient conditions to impact device stability [4].

In this review, we shall analyze the various structures of PSCs (Fig. 1) that employ the usage of MO, certain MO materials used, corresponding performance and stability values obtained, and strategies to improve performance and prospects.

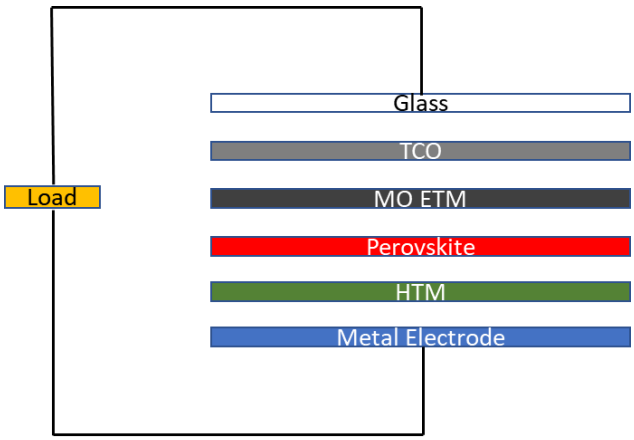

Fig. 1. PSC Architecture

PSC Architectures

The PSC structures can be broadly divided into planar and mesoporous categories (Fig. 2). The structures have specific board differences. As the name suggests, the mesoporous architecture includes a mesoporous semiconductor layer that behaves as a scaffold layer whilst acting as the electron transport material. Planar architectures are further divided into inverted and normal. The planar configuration is n-i-p, where n is the ETM, i is the active layer, and p is the hole transport material (HTM). The inverted architecture has a p-i-n configuration. MO ETMs have been used extensively with reasonable and commercial possibilities in both these structures.

In hybrid PSCs, a MO ETM is one of the most vital layers that is incorporated into the fabrication of the device. Different materials are used as the compact MO ETM layer (varies according to the lab). The point to note here is that it is not just the perovskite film quality that

matters but also the charge transport materials. The importance of the ETM is of even more significant concern when considering both low and high-efficiency devices.

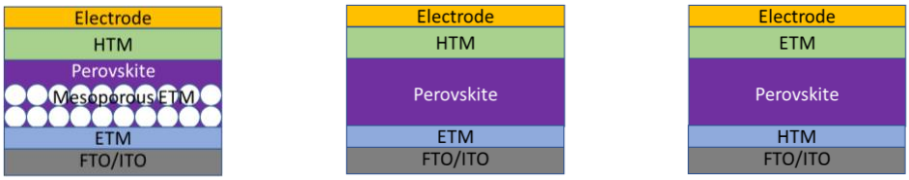

a) b) c)

Fig. 2. PSC Typical Architectures: a) Mesoporous, b) Regular, c) Inverted

Planar Structure

MO-incorporated planar devices have yielded efficiencies similar to the mesoporous structure. It has reached a point where both these structures are competing for commercial activity. The highest recorded efficiency using an MO ETM in a planar PSC is 23.7% [5]. In the conventional n-i-p structure, mesoporous MOs are essential as a scaffold and fast-charge transport material. In this configuration, the MO has a large contact area with the perovskite layer, producing highly efficient devices. This is why researchers often prefer this architecture while fabricating MO-based PSCs.

Planar structures have been at the forefront of developing rapid and high-efficiency values. However, they are victims of hysteresis, which impacts device stability in the long run. Identifying the root cause of hysteresis is necessary to quantify the absolute value of PCE. The most robust method of identifying the PCE value is by estimating electron current density and hole current density. A balance needs to be established between these two parameters. A deviation from this balance can be associated with recombination through radiative or non-radiative methods.

Mesoporous Structure

In this structure, similar to the name, there is a mesoporous MO used. Typically, TiO_2 is the mesoporous layer used. Some unconventional materials like ZnO, SnO_2, ZrO_2 and Al_2O_3 have been used as the scaffold ETM layer [6-9]. Current research is going on in varying the ETM/perovskite interface, improving surface morphology, modifying interface compatibility, and optimising charge transport (Fig. 3).

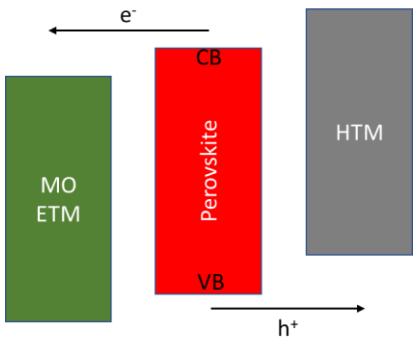

Fig. 3. Energy band alignment of PSC components

A mesoporous structure is an ideal fit to replace the planar structure and eliminate the hysteresis phenomenon. The mesoporous MO layer provides a larger contact area which facilitates faster and smoother charge transfer and sets a precise balance between both charge carriers (Fig. 3). A technique that can improve the performance and stability of the device is by tuning the geometry and structure of the mesoporous MO layer [10-13].

Electron Transport Material (ETM)

The function of an ETM is to decrease the energy barrier between the electrode and the perovskite layer. Moreover, it helps transport the electron from the active layer to the external load via the cathode. Understanding the extraction, transportation and collection processes to produce high-performance PSCs is crucial. There are specific requirements that need to be met by an ETM, including a) high transparency, b) suitable energy band alignment with the perovskite layer, and c) high electron mobility [14]. ETMs can be broadly divided into two categories: A) inorganic materials, which include MO and materials that do not include common degradable materials like ZnO, TiO_2, SnO_2, In_2S_3, WO_3, CeO_2 and $SrSnO_3$. These are materials that are affordable and commonly available either commercially or can be sourced. B) Organic materials are carbon-containing compounds like PCBM and PDI that are expensive but produce efficient devices.

An ETM is considered suitable for a device post deliberating over certain essential factors [14]. While depositing a perovskite layer on the ETM, it is essential to see its impact on grain size and several lattice defects. Suppose the existing ETM can promote more excellent crystallinity for the perovskite layer whilst passivating defects. In that case, there is a considerable advantage for that device. Moreover, there needs to be an energy band alignment with the perovskite and the subsequent layers in the device. The bandgap can be tuned when attaching the charge transport materials to the perovskite layer. The crystallization of the perovskite layer should be different from the compact ETM layer.

The advantages of using an ETM are pretty evident: a) protects the device against extrinsic factors, b) provides added chemical, thermal and mechanical stability, c) facilitates movement of carriers to the electrodes, and d) restricts recombination by blocking holes. Thus improving device performance.

MOs as ETMs

Inorganic ETMs are regarded for their quick transfer of electrons and small refractive index. The application of MOs has been spread across PSCs, dye-sensitized solar cells (DSSCs), optical devices and more. MO ETMs are an integral part of the PSC, and it goes beyond the usage of just the transfer of electrons. Ideally, along with being an efficient charge collector, it should provide a short diffusion length and promote crystallinity/crystal growth of the perovskite layer.

When an ETM (particularly MO ETM) comes in contact with a transparent conductive oxide (TCO), specific requirements must be fulfilled before fabricating the device. Firstly, a built-in voltage (V_{bi}) is of utmost importance. This potential aids in charge separation and transport, eventually contributing to V_{oc}. The V_{bi} depends on the depletion region formed. To further improve the V_{bi} value, it is essential to tune the Fermi levels. Researchers were capable of tuning Fermi levels by surface engineering, molecular engineering, doping and particle size tuning techniques [15,16]. The depletion zone width is also an important aspect that impacts device performance. The permittivity of MOs is another factor that needs to be considered, as it correlates with the carrier concentration and the depletion region width [15].

Secondly, a Schottky Barrier phenomenon develops when an ETM comes in contact with a TCO [17]. This essentially implies that there is an energy barrier between an electrode and a charge-transporting material that a charge carrier needs to overcome. Only upon eliminating this charge barrier will PSCs be able to reach their highest possible efficiency. Currently, not

many active methods are prevailing to eliminate the barrier. However, doping with metal ions has proven to be an effective strategy for developing high-efficiency PSCs.

A MO ETM (Fig. 4) has vital characteristics like stability and limited hysteresis. However, a MO suffers oxygen vacancies and surface defects. During operation and voltage-current scans, this gives rise to anomalous hysteresis results. Hence, it is necessary to passivate the MO layer though chloride treatment of polymer layers, potentially reducing these defects [18,19].

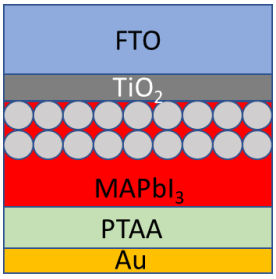

Fig. 4. Device architecture of mesoporous TiO_2 PSCs

Deposition Methods

While using MO as ETMs (doped or undoped), certain limitations come with it, like figuring out a suitable fabrication process that can be commercialized and the degree of crystallinity and morphology of the produced film. Several studies study the stability and reproducibility of MO ETMs and focus on the root cause of degradation mechanisms in the fabricated device.

The end goal while using MO ETMs goes beyond reducing fabrication costs and device efficiency. Instead, it should focus on how these devices can be brought up to scale and commercialized. It is safe to consider that, while using MO ETMs in PSCs, advantages like low costs, good transparency, improved stability and appropriate charge transfer properties are easily attainable. However, the real challenges arise when a) inevitable electrical properties of MOs, b) poor interfacial contact with the perovskite layer, c) unpredictable stability performance characteristics under real-world conditions, d) high recombination sites at the perovskite/ETM interface, e) high resistance to extrinsic and intrinsic stability factors [1].

The method through which MO is deposited and allowed to grow on a substrate is highly essential. Various methods and processes yield MO films with different morphologies, surface compatibilities, and conductivities. The deposition methods can be vastly classified into solution-processed and atomic layer deposition.

Solution Process

Solution-processed MO ETMs are the most common form of synthesis. This is done through either thermolysis, nanostructures or other auxiliary methods. The thermolysis method includes spin or spray coating metal hydrates or salts dissolved in suitable solvents. These substrate-coated films are then thermally annealed to form the MO ETM. In the case of nanoparticles, methods like screen printing, slot-die coating and spin coating have been actively used. Screen printing is a method which uses a mesh that helps in switching from a paste format of MO onto a flat substrate [20,21]. Slot-die coating is an excellent method that helps produce homogeneous and wet films without any unnecessary contact, especially for flexible substrates. It is important to note that films produced through solution-processed mechanisms are susceptible

to temperature and humidity. There are other derivative methods of solution process like sol-gel, sonochemical, chemical precipitation, spray pyrolysis and chemical combustion [22-24].

Atomic Layer Deposition Process (ALD)

This subset of Chemical Bath Deposition (CBD) is a crucial technology for producing thin and uniform films. In this method, precursor A is allowed to enter a gas chamber to permit chemisorption and produce a thin film on the substrate. The excess and unreacted components are then purged. Precursor B is allowed to enter the gas chamber and then reacts with A to form an ultrathin film [25,26]. Similarly, the excess and unreacted components are purged. This method produces uniform-thickness films which are compatible even on rough surfaces. ALD has been previously used for ZnO, TiO_2 and SnO_2. However, its complex mechanism and high costs have limited the usage of this method.

Chemical Bath Deposition Process (CBD)

In this method, substrates are immersed in a solution of the metal's hydroxides, sulfides or selenides to form the MO ETM [27]. Typically, this method is used to produce buffer layers in PSCs. However, in recent years, this method has been used to deposit ZnO and SnO_2. Some notable advantages of this method include low-temperature processing, commercial and low costs. In contrast, the films produced through this method heavily depend on the precursor solution's pH, growth conditions, temperature and concentration [28].

Mechanosynthesis of MO ETMs

This method is typically used to produce low-dimensional MOs. It includes the preparation of the MOs through physical grinding. This clean, low cost and high-yield method results in highly pure and crystalline MO outputs. The process can be broadly described where a three-dimensional material undergoes a wet milling procedure and is broken down into lower dimensions like nanoparticles, nanorods, nanosheets, etc. [29,30]. In order to obtain the various morphologies, the milling conditions need to be regulated. This method has been actively used to produce SnO_2, TiO_2 and NiO_x. The method produces a compact charge transport layer through a low-temperature process. The output is then deposited using methods like spin-coating when the nanomaterial is dispersed in a solution.

Auxiliary Processes

Hydrothermal processes are a category that produces low-temperature processing and adhering solid films. Hong and co-workers used this method to produce TiO_2 MO ETMs and ALD-processed TiO_2 as a passivation layer [31]. Electrodeposition (ED) is another vital method. As the name suggests, electricity is used to deposit a thin film on a given substrate. Wei and co-workers used a similar strategy where $TiCl_3$ was electrodeposited to form TiO_2 ETM with a device PCE of 13.6% [32]. This method allows one to effectively tune and regulate the thickness of a film being deposited. The combustion method is another standard process used. In this method, an oxidizer chemical is placed on a substrate along with fuel to produce a uniform and smooth film on the substrate. Facchetti and co-workers used this technique to produce stable and efficient ZnO films with a device performance more significant than 20% [33].

Physical deposition processes like magnetron sputtering, electron beam evaporation and pulsed layer deposition are also viable methods with great possibilities to produce flexible devices. However, these methods are costly and time-consuming [34-36].

Physical Vapour Deposition (PVD) and Chemical Vapour Deposition (CVD) techniques involve high costs, high energy inputs and complex prerequisites. Various methods come under CVD and PVD, including coupled and derivative methods, which are inaccessible and more expensive than other processes.

Requirements of a MO ETM

Every component in a PSC is required to fulfil specific characteristics. However, coming to the case of MO ETM, additional criteria need to be fulfilled, like the optoelectronic properties, material compatibility, morphology and stability. The suitable energy band alignment between charge transport materials is essential to obtain high-efficiency devices. The conduction band minimum of the ETM needs to be lower than the conduction band of the perovskite. Similarly, the valence band maximum of the HTM needs to be slightly higher than the valence band of the perovskite layer. It is important to note that there needs to be a sufficiently high energy barrier between the perovskite and ETM, which helps in efficiently blocking holes and reduces charge recombination. The built-in voltage (V_{bi}) is determined by the charge transport material and the perovskite. In this case, the higher the value of Vbi, the higher the value of V_{oc}, as the material can separate the charges to a greater extent and improves charge transport. Much research in the interfacial engineering domain aims to reduce charge recombination and improve J_{sc}, V_{oc} and PCE values.

Carrier mobility is another vital aspect that directly impacts charge carriers' transport. There needs to be a significantly high carrier mobility value which restricts the charge accumulation at the interface and reduces hysteresis. Moreover, the material must have a wide bandgap with a small refractive index. The morphology of the MO ETM is a factor that is often neglected. It is regarded that a morphology for the ETM should be selected on the following basis, a) promote perovskite crystal growth, b) helps in the further coating of device layers, c) improves perovskite film surface coverage, and d) eliminates shunting pathways.

The interfacial quality between the perovskite and ETM determines film quality, PCE and device stability. Further research is being carried out in this area to look after the perovskite/ETM interface and produce a smoother ohmic contact between the ETM and the electrode. Moreover, MO ETMs should also have excellent stability properties to UV light exposure and have low photocatalytic effects to contribute to the stability of the device. MO ETMs are often used for their improved stability properties against moisture and as protection layers to prevent perovskite degradation. Currently, research is being carried out on how these devices' thermal and chemical stability can be further optimized and obtain a longer device lifetime. A few other notable criteria are mentioned below.

Electronic Properties

The conduction band of the ETM needs to be suitably aligned with the perovskite active layer. This ensures that there is efficient electron extraction, transport and conversion efficiency. As a result, the short current density (J_{sc}) is improved. The valence band must be placed sufficiently lower than the perovskite layer to ensure efficient hole blocking. The more significant difference between the valence and conduction band levels, the more significant will be the open circuit voltage (V_{oc}) and fill factor (FF) values [37].

Electronic properties are not limited to energy band alignment but delve into the material properties. It is more than a necessity that each considered MO ETM has sufficient electron transfer mobility, electron collection properties and limited charge recombination [38]. MO ETMs also need to behave as a passivating layer that can reduce interfacial and structural defects.

Optical Properties

Essentially, any ETM should be as transparent as possible. This would increase transmittance and not lead to any parasitic absorption. It would be beneficial if these materials had a wide bandgap, high transmittance and a small refractive index. The MO ETMs also need to be extremely stable to UV and other deteriorating radiations. It is responsible for no degradation of the active layer [39].

Morphology Control

The surface morphology of an ETM is essential as it directly or indirectly impacts the device's performance. A film with good morphology can facilitate smoother interfacial contact between the perovskite and the charge transport material. This further supports smoother electron transfer, collection and mobility through the layers. Furthermore, a smooth film with appropriate morphology will not have pinholes and be dense [5].

Chemical Stability

An excellent ETM is expected to have impeccable stability properties. Moreover, it should not involve any interaction with the adjacent perovskite layer. To be highly stable, the MO ETM should be hydrophobic and non-hygroscopic to prevent perovskite degradation (Fig. 5).

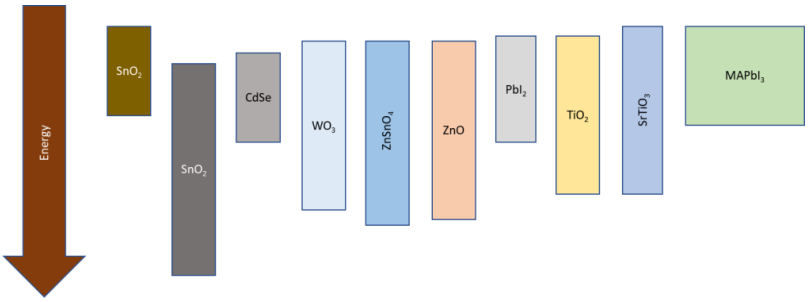

Fig. 5. Energy band alignment of various MO ETMs

Standard MO Materials used as ETM

TiO_2

The most renowned and widely used MO ETM is TiO_2. Undoubtedly, its superior stability, electrical and optical properties, and suitable energy band alignment make it a very favourable material. Miyasaka and co-workers used a nanocrystalline TiO_2 that behaves as an ETM and a supporting layer. Mesoporous TiO_2 (mp-TiO_2) is a material constantly being researched for thickness optimization and scaffold ability. A printed PSC using TiO_2 attained a PCE of 12.8% and 1000 h of stability under 1 Sun of complete illumination [7].

Grätzel and co-workers incorporated Cs and Rb into the perovskite lattice to get efficiencies greater than 20% using TiO_2 as an ETM [40,41]. Seo and co-workers used mp-TiO_2 and P3HT as the ETM and HTM, respectively, to produce a PCE of 22.7% [42]. Snaith and co-workers synthesized TiO_x from titanium isopropoxide to yield reasonably high efficiencies for an inverted configuration [43]. Conings and co-workers developed a low-temperature processible TiO_2-based ETM from a one-step nanoparticle setup for planar PSCs [44]. Kim and co-workers discovered an ALD method to synthesize TiO_2, which does not require thermal annealing and is compatible with planar PSCs. Plasma-enhanced ALD to produce a TiO_2 ETM requires thermal annealing at only 80 ^oC with an efficiency retaining ability more remarkable than 90% [45]. Yella and co-workers used a low-temperature method to produce TiO_2 using a nanocrystalline approach. This technique showed how one could increase the interfacial area to support smoother charge transfer and improved charge extraction with a device efficiency greater than 13% [46]. Chen and co-workers used an RF magnetron sputtering to depose TiO_2 on a substrate [47].

Different forms of TiO_2, like anatase and rutile, have also been used as ETMs. Anatase-based devices have produced an efficiency of 9.9%, and rutile-based devices have an efficiency of 11.8%. There are studies where both phases have been combined to obtain the merits of both phases. Using the anatase/rutile arrangement produced an efficiency greater than 15%, while the rutile/anatase arrangement produced a slightly higher efficiency. This can be related to why

rutile/anatase arrangement greatly facilitates electron transfer. In contrast, the anatase/rutile arrangement produces a barrier for electron recombination [48].

TiO_2 can be synthesized through pyrolysis, thermal oxidation, ALD, CBD, electrodeposition and the most common spin coating method. The thermal oxidation formed TiO_2 film is smooth, compact and can be sintered simultaneously. The ALD process is suitable for flexible substrates. However, it requires high processing temperatures, and thickness plays a crucial role. Current research is being focused on how processing temperatures can be reduced. Lv and co-workers developed a TiO_2 ETM using the ALD process. The produced film was pinhole free and had nearly no impact on perovskite degradation. TiO_2-produced through the ALD method is low-temperature processed, reduces charge recombination, and has improved stability [49].

The morphology of TIO_2 also plays a significant role in how the device performs. Gao and co-workers produced TiO_2 nanoparticles and nanotubes. The study found that the morphology impacted the device performance with a significant difference in J_{sc}, V_{oc}, FF and PCE values.

However, TiO_2 is regarded for its severe electron accumulation at the perovskite/ETM interface, resulting in severe hysteresis. It also shows low bulk electron mobility, high processing temperatures, and post-treatment thermal annealing that requires researchers to scavenge for more fantastic alternatives.

SnO_2

SnO_2 is a very plausible alternative to TiO_2, considering its wide bandgap, small refractive index and improved bulk electron mobility. These features and suitable energy band alignment enable SnO_2 to support easier charge extraction, transport and collection. Tian and co-workers used SnO_2 nanoparticles to produce a PSC using spin coating with a PCE of 13% [50]. Dai and co-workers used a SnO_2 compact layer produced through high-temperature processing to get an efficiency of around 6% [51]. Fang and co-workers used $SnCl_2.2H_2O$ to synthesize SnO_2 through a low-temperature pyrolysis method. The device produced 17.2% PCE [52]. The low-temperature processes and high-efficiency results of SnO_2-based PSCs produce more devices using this method. Jen and co-workers synthesized hydrothermally generated SnO_2 nanoparticles with an efficiency greater than 18% and improved stability [53]. Hagfeldt and co-workers combined spin coating and chemical bath deposition methods to synthesize a modified SnO_2 ETM with an efficiency close to 21% [54]. Mahmood and co-workers showed how SnO_2 nanosheets could be produced through a one-step deposition method to produce reduced hysteresis devices, better charge collection and stability properties [55]. Anaraki and co-workers fabricated a planar PSC with a PCE of 21% using SnO_2 as the ETM synthesized through CBD [56].

Ke and co-workers determined a low-temperature solution-processable method to produce SnO_2. This method was highly reproducible as it was tested on 30 solar cells to yield a maximum efficiency of 16.44%. This is due to the excellent SnO_2 structure, hole-blocking ability, high transmittance and wide bandgap [57]. Baena and co-workers synthesized a SnO_2-ETM through a low-temperature ALD process with an efficiency greater than 18% [58]. Subbiah and co-workers developed an innovative method to produce SnO_2 ETM at low temperatures [59]. In this case, the precursor solution was activated using an N_2 RF plasma, forming an internal metal-oxide framework. This further facilitated device performance as efficiency of 20.3% was recorded on rigid substrates and 18.1% on flexible substrates. Bu and co-workers used a slot die coating method whereby a very feasible method was used to fabricate printable PSCs [60]. Moreover, this strategy suppressed hysteresis and efficiency greater than 17% and 15% for large-area PSCs.

SnO_2 has inevitable significant downfalls like intense charge recombination and accumulation. Moreover, the higher trap density behaves as recombination sites, further limiting device performance. Recently the usage of SnO_2 in planar PSCs has been promoted, and the highest recorded efficiency is nearly 23%.

ZnO

ZnO has a similar structure to TiO_2 and is used in the form of solutions or nanostructures. ZnO has suitable bulk electron mobility, energy band alignment and high transmittance to visible light. Hagfeldt and co-workers used ZnO nanorods in a mesoporous PSC to obtain a PCE of 5% [61]. Kelly and co-workers used ZnO processed at low-temperatures to form a compact layer with minimal surface roughness, uniform thickness, and a sizeable crystalline device with a PCE of 15.7% [62]. However, the nature of ZnO is highly unpredictable. An underlying chemical reaction takes at the ZnO/perovskite interface, which does not produce a suitable perovskite film. Lai and co-workers developed radio frequency sputtered ZnO to get a PCE of nearly 11% in an inverted PSC configuration [63]. Yang and co-workers developed low-temperature processed ZnO nanoparticles with a considerably higher J_{sc} value than its PCBM counterpart [64]. It was also observed that the ZnO-based device possessed improved stability because the ZnO layer was a diffusion barrier for the metal electrode ions into the perovskite. Tang and co-workers synthesized a ZnO nanowall through a CBD method [65]. This reduced charge recombination improved charge transfer and collection and increased device performance. Similar to TiO_2, the morphology of ZnO plays a vital role in device performance. ZnO nanotubes and nanocrystals-based devices resulted in different PCE values. Park and co-workers developed a method to use undoped ZnO. They only used optimisation and engineering techniques to produce a PCE of 11.3% [66]. Compact ZnO (c-ZnO) is a fantastic candidate for ETMs. However, the basic nature of ZnO deprotonates the Methylamine (MA) cation resulting in MA loss, which leads to the formation of PbI_2. The process further accelerates because of the hydroxyl or acetate groups present (Fig. 6).

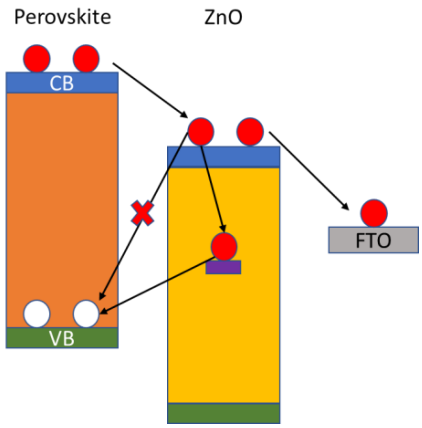

Fig. 6. Energy Band Diagram representing Capturing/Scattering Process

Liu and Kelly used ZnO nanoparticles to synthesize the corresponding ETM, produced from Zinc Acetate Dihydrate and Potassium Hydroxide [67]. This method depicted how room-temperature processed materials can be developed with appropriate crystallinity and dense nature without any heating requirements. Once the film was optimized with the required thickness and adjusting the surface roughness, the device yielded an efficiency greater than 15% for rigid substrates and 10% for flexible substrates. Song and co-workers again used ZnO nanoparticles. However, the Formamidine cation was used instead of the traditional MA cation to overcome the stability issue [68]. The ZnO-$FAPbI_3$-based device resulted in a PCE of 16.1% with improved stability characteristics. The $FAPbI_3$ was then replaced with a triple cation perovskite material, and the resulting device had a PCE greater than 18%.

Moreover, the triple cation fabricated device depicted superior stability characteristics (chemical, mechanical, thermal and environmental). Yang and co-workers developed a PSC

device through a solution-processable method using a Zinc complex containing hydroxyl groups [69]. This eventually reduced the device annealing temperature, improved the V_{oc} value, delivered a PCE greater than 16% as an ETM and offered impeccable stability. Using a low-temperature approach, Mathews and co-workers synthesized a compact ZnO film through electrodeposition and ZnO nanorods through CBD [70].

Zhang and co-workers developed a Metal-Oxide-Framework (MOF) based on ZnO [71]. This structure improved charge extraction and reduced traps, where the perovskite layer filled the pores of the framework. This increased the light-harvesting efficiency and improved charge transport characteristics. Mahmood and co-workers developed ZnO nanosheets to produce an efficient and hysteresis-free device with a PCE of nearly 16% [72]. Using a similar approach, Mahmood and co-workers developed ZnO nanodisks and nanowells. The nanowells morphology possessed a unique characteristic where holes were grown perpendicular to the substrate, which increased surface area for better charge transfer. The device fabricated using the nanowells approach was 16.65%.

As mentioned previously, the interface stability at the ZnO/perovskite layer is concerning. Moreover, there is an intense charge recombination case in the case of ZnO-based devices. However, the reasons go much beyond this. The optimum performance of ZnO is obtained only at high temperatures (> 400 ^{o}C), which calls for modified synthesis procedures. There has been an alternative synthesis method with processing temperatures near 290 ^{o}C. However, this is a temperature which is not ideal for flexible substrates.

Fe_2O_3 (Hematite)

Hematite is an up-and-coming ETM with peculiar electronic properties, improved chemical stability, and low cost. It was previously used in other optical and optoelectronic devices. Hong Lin and co-workers used Fe_2O_3 and conducted a comparative analysis with TiO_2 as the ETM [73]. It was noticed that Fe_2O_3 had improved charge extraction properties, lower recombination rates, reduced hysteresis and enhanced stability properties.

However, with its reduced electron mobility and visible light absorption properties, the device performance using Fe_2O_3 is not optimum and is subject to further improvement.

Zn_2SnO_4

Zn_2SnO_4, commonly referred to as ZSO, has a wide bandgap, low refraction index and high electron mobility. Its energy band shows similarities to TiO_2 and enhanced stability properties, making it a very capable ETM. Oh and co-workers used a device containing ZSO nanoparticle-based ETM to produce a PCE of near 7% [1]. Shin and co-workers synthesized ZSO nanoparticles using hydrazine at 100 ^{o}C [74]. The nanoparticles could yield a PCE of 15.3% for flexible PSCs applications. Wu and co-workers produced a homogenous and dense film of ZSO to obtain a PCE greater than 16% [75]. ZSO has excellent optical transmittance, hole-blocking ability, energy band alignment and efficient charge transportation and collection properties. Using these advantages of the material, Jun and co-workers developed a solution-processable ZSO film with a mixed perovskite active layer [76]. The fabricated devices yielded a PCE of 20.02% with improved stability and minimal hysteresis properties. Tavakoli and co-workers used an ultrasonic spray pyrolysis-assisted method to deposition ZSO nanorod arrays [77]. The device yielded a PCE of 18.24% with J_{sc} greater than 23 mA/cm^2 due to better charge extraction and reduced hysteresis.

Kim and co-workers developed ZSO nanoparticles with a PCE greater than 7% [78]. Jen and co-workers synthesized ZSO nanoparticles using a hydrothermal method which was later coupled to form PCBM/ZSO [79]. This arrangement yielded greater than 17.76% with excellent stability against the ambient environment. Although possessing suitable characteristics, obtaining ZSO nanoparticles or synthesizing it as an ETM, lowering its costs and commercializing it are just a few of this material's disadvantages.

$BaSnO_3$

$BaSnO_3$ (BSO) is a material with a suitable conduction band position and high electron mobility. Dai and co-workers used BSO as an ETM in a mesoporous PSC with a PCE of 12.3% [80]. The structural similarity between $BaSnO_3$ and the perovskite layer facilitates charge transfer and J_{sc}. Guo and co-workers produced BSO nanoparticles through a precipitation method [81]. Zhu and co-workers used BSO nanoparticles in a device to yield a PCE greater than 12% [82]. The mobility of BSO-based ETM can be improved by metal doping, particularly La-doping. The produced material is then La-doped BSO (LBSO). Zhu and co-workers used LBSO to obtain a PCE greater than 15%. However, to synthesize LBSO, we need temperatures greater than 700 ^oC, which is not at all viable. Shin and co-workers fabricated LBSO-ETM below 300 ^oC with excellent stability properties and a PCE of 21.2% [83]. Sun and co-workers used BSO nanoparticles through a peroxide precipitation method. The processing temperatures were reduced to 150 ^oC, and a PCE of nearly 11% was achieved [84].

Hong Lin and co-workers used BSO and PCBM in an inverted configuration to yield 16.2% PCE [85]. The device also possessed stability characteristics where it retained 90% of its initial PCE after 600 h of ambient environment storage. Some notable disadvantages of this material include incredibly high processing temperatures and charge recombination rates.

Other MO ETMs

WO_x (Tungsten Oxide) is another considered ETM due to its high electron mobility and wide bandgap. Amassian and co-workers synthesized WO_x nanosheets and obtained a device PCE of 3.80% [86]. Ma and co-workers improved the PCE of WO_x-based devices by greater than 10% using a low-temperature solution-processed technique [87]. It was observed that most WO_x-based devices had higher V_{oc} and FF but lower J_{sc} values. This can be related to the fact that WO_x suffers from severe charge recombination. Chen and co-workers deposited a nanocrystalline WO_x ETM layer by reaction of Tungsten Chloride with Hexanol, with a processing temperature of 50 ^oC [88]. The Hexanol aided in tuning the energy band suitably and reducing charge recombination. The perovskite used in this case is a mixed molecule with a PCE of 20.77%.

Niobium Oxide (Nb_2O_5) is another considered ETM due to its improved chemical stability and appropriate electronic and optical properties compared to TiO_2. Miyasaka and co-workers showed how replacing TiO_2 with Nb_2O_5 produced a device with higher V_{oc} and more significant hole-blocking properties [89]. Liu and co-workers used Nb_2O_5 on large-area PSCs using an electron beam deposition method with a PCE greater than 18% for planar PSCs [90]. They also concluded that the device performance was susceptible to the thickness of the Nb_2O_5 layer and how this material paved the way for large-area devices. Feng and co-workers suggested synthesizing Nb_2O_5 through electron beam evaporation is an excellent candidate for flexible ETMs [91]. Jiang and co-workers used ethanol ruthenium to prepare a coupled ETM of TiO_2-Nb_2O_5. The device using this material produced a PCE of 15.25% [92].

Moreover, the film is exceptionally smooth, supports charge transfer and has high charge mobility. Gu and co-workers fabricated a device using spin-coated Nb_2O_5 where the V_{oc} value was 1.2 V. The J_{sc} value was 21.63 mA/cm^2 [93]. These high photovoltaic output values can be associated with reduced interfacial recombination and high transmittance value. Erenow, Ling and co-workers used an RF magnetron sputtering method to deposit amorphous Nb_2O_5 at room temperature [94]. The high mobility and conductivity of the film yielded a device efficiency of 17.2%. Wang and co-workers synthesized Nb_2O_5 nanoparticles which were solution-processable and low-temperature processed with a PCE greater than 20% [95]. The well-aligned energy bands helped charge extraction and injection with reduced transfer losses. On exposing the device to UV light for 10 h, 93% of the initial J_{sc} was still retained.

Cr_2O_3 is a promising ETM with its suitable energy band alignment and remarkable stability characteristics. The highest obtained PCE using Cr_2O_3 is above 16%, which can be

compared to TiO_2-based devices. However, Cr_2O_3 has higher series resistance, which further limits the FF and PCE of the device.

Cerium Oxide (CeO_x) is a potential ETM because of its wide bandgap, high ionic conductivity and enhanced stability (thermal and chemical) properties. Deng and co-workers developed a CeO_x-based device with a PCE of 14.32% using a low-temperature processing approach [96]. Chen and co-workers used a solution-processed CeO_x in inverted PSCs with a PCE greater than 17% [97]. CeO_x has an added advantage, where incorporating its film into a device can also behave as a diffusion barrier for metal ions and an extrinsic environment barrier.

Ye and co-workers used $NaTaO_3$ as an ETM [98]. In this case, $NaTiO_3$ was capable of passivating the excessive trap sites, preventing perovskite degradation and improving stability characteristics. The device produced an efficiency greater than 21%, where even after 240 mins of UV exposure, 80% of its initial PCE was retained.

In_2O_3 is another potential candidate to produce efficient PSCs due to its wide bandgap, high electron mobility and good transmittance properties. Chen and co-workers produced a solution-processable and low-temperature In_2O_3 ETM with good film morphology and PCE greater than 15% [99]. In_2O_3 shows lower photocatalytic activity than TiO_2, implying that the perovskite layer will be much more stable in the former case. After exposing to a dark environment for three months, the device retained 94% of its initial PCE. Yoon and co-workers formed a pinhole-free In_2O_3 film by spin-coating a complex between Indium Oxide and water [100]. The obtained film showed improved conductivity and reduced surface roughness.

Due to their unique electrical and optical properties, ternary metal oxides possess an extremely bright future in the PSC industry. These properties can even be tuned with the modification in cations. The major challenge lies in developing a low-temperature processing method which can effectively commercialize these materials. However, it is essential to note that along with having peculiar ternary metal oxides, research and improvement on existing MOs like TiO_2 should continue to tune their properties even further. Ternary oxides like BTO, STO and Ti-Fe-O have been reported and used to produce effective devices. Suzuki and co-workers used BTO as an ETM in a mesoporous architecture to get a PCE of 12.4% [101]. STO is known for its high electron mobility and dielectric constant, making it suitable for a mesoporous ETM. The first mesoporous STO device produced a PCE greater than 7% [102]. Ti-Fe-O compounds have combined benefits of TiO_2 and Fe_2O_3. Hong Lin and co-workers used $Ti_{0.5}Fe_{0.5}O_x$, which showed improved charge extraction, transport abilities and reduced hysteresis, with a PCE of 14.7% [5]. However, the large surface area of this material does not provide a sufficient surface area which reduces the J_{sc} value of the device. Bera and co-workers used $SrTiO_3$ as an ETM to fabricate a device [103]. The molecular structure of $SrTiO_3$ heavily resembled a perovskite structure. Eventually, the device produced a PCE of nearly 7%. Neophytou and co-workers used a low-temperature method to deposit $SrTiO_3$ [104]. The resulting device yielded a PCE of 19%, with a retaining efficiency power of 80% under 1000 h of illumination.

Gu and co-workers used $ZnTiO_3$ in planar PSCs due to its excellent photostability and minimal photocatalytic activity [105]. The device fabricated using this material produced an efficiency of 19.8%. After UV soaking results for 100 h, the device retained 90% of its initial PCE. Wang and co-workers tuned the ferroelectric properties of $PbTiO_3$ to improve photocurrent and PCE values [106]. The tuning in ferroelectric properties improved charge extraction and reduced charge recombination with a PCE of 12.28%. Other auxiliary Ti-based ETMs have also been developed, like $Zn_2Ti_3O_8$ and $BaTiO_3$. However, these devices had very low efficiencies because of their low mobility values and poor energy band alignment. Ternary metal oxides containing Sn are considered revolutionary candidates for ETMs due to their best positioning of conduction band maximum with the perovskite layer.

Strategies to Improve Device Performance

Although MO ETMs have unique and remarkable advantages, it comes with their fair share of disadvantages. In order to fabricate high-efficiency PSCs using MO ETMs, it calls for strategies and techniques that can either tune the properties of these layers or minimize the disadvantages to a greater extent. In this section, we shall look into some of the commonly used strategies that can optimize MO ETMs.

Nanostructure Design

MO ETMs in PSCs are stuck to the device (adhere). In some cases, the device forms from irregular film coverage, poor charge extraction and charge transport. Fang and co-workers developed a two-step low-temperature method to produce SnO_2 quantum dots (QDs) [107]. It was observed that SnO_2 QDs resulted in improved film coverage and optical transmission, formed more compact layers, and had a narrower size distribution than nanocrystal-based ETMs. These advantages eventually improved the device's performance. Wang and co-workers designed a unique method to produce Fe_2O_3 nanoisland-based ETM [108]. The device PCE was improved from 14.82% to 18.2% due to its reduced charge recombination and improved charge extraction and collection. Wang and co-workers used $SrTiO_3$ nanoparticles with graphene [109]. As a result, the device PCE obtained was 10%, with an improvement of J_{sc} from around 12 to 18 mA/cm^2.

Mesoporous structures using MO nanoparticles suffer from drawbacks such as poor pore filling, electron transport, high trap density, and defects. Various nanostructures, like nanorods, nanosheets, nanowires and nanocones, have been developed to overcome these issues. The main aim of these structures is to fulfil direct and capable charge transfer channels between the perovskite and ETM. This eventually improves light harvesting and conversion efficiency to improve device performance. Park and co-workers used ZnO nanoparticles and tuned its length and diameter [110]. This was achieved by modifying the precursor concentration and immersion time. The ZnO-based devices obtained from this method yielded an efficiency greater than 11%.

Huang and co-workers developed SnO_2 nanorods for mesoporous PSCs, improving stability and operational efficiency by 16.57% [111]. The principal reason for having nanostructures is to improve electrical and optical properties to produce high-efficiency PSCs. Caruso and co-workers synthesized TiO_2 and SnO_2 nanosheets to conduct a comparative analysis [112]. The SnO_2 device showed better performance due to its reduced charge recombination and improved charge transfer.

Hong Lin and co-workers used ZnO nanocones through the CBD synthesis process [113]. The ZnO nanocone layer was coated with an additional ZnO thin layer to behave as a capping film. This arrangement produced a PCE greater than 18% and enhanced thermal stability.

Elemental Doping

Doping is one of the most effective strategies that has been actively used to regulate the electronic properties of MO. There are two common types of doping: n-type doping and p-type doping. The former case uses higher valence elements, and the latter uses lower valence elements [5].

P-type doping passivates and reduces the number of defects, trap states and surface trap density on the MO surface. Moreover, doping using these elements adjusts the energy band and a sufficient shift in the CB. This further improves charge transfer, extraction, reduced charge recombination and eventually improved device performance and stability. In the past, Mg and Y and In-doped TiO_2 have been used to tune energy band levels and improve electron transport, which has led to an increase in V_{oc}, J_{sc} and PCE of the device. Nd and Sn doping has also helped to enhance the device's performance and stability. This is because of its ability to reduce surface defects and recombination. Ginger and co-workers showed how Zr-doped TiO_2 improves device performance by increasing electron lifetime and transport properties [114]. N-type doping increases J_{sc} values, charge extraction, collection and transportation. Jung and co-workers showed how Nb-doped TiO_2 improved electron injection properties [115].

Metal doping of TiO_2 can improve the photovoltaic parameters of the material as it improves electrical conductivity, energy band alignment, light harvesting efficiency and carrier mobility. TiO_2 doped with Ru nanoparticles have yielded smoother and improved films. Graphene-decorated TiO_2 improves the device's stability, reducing series and contact resistances. Ag-doped TiO_2 improves the energy band position, and the device performance difference can be observed through an undoped TiO_2-based device. Feng and co-workers showed how La-doped TiO_2 efficiently improves device performance [116]. La has a strong bonding towards oxygen, and this helps in improving device structure and stability for more effortless charge transfer and reduced charge recombination. Europium and Samarium doping of TiO_2 is also being extensively considered, as incorporating these rare earth materials improves light absorption in longer wavelengths. Zhang and co-workers used Eu and Sm-doped TiO_2. They observed improved stability, lesser degradation of the perovskite layer, modification in energy band alignment, and more significant absorption in longer wavelengths [117]. This eventually resulted in a device efficiency of 19.01%. Doping of TiO_2 using promising materials like Erbium, Ytterbium and Niobium has shown improved absorption characteristics in the NIR region. Zhou and co-workers also used Cadmium-doped TiO_2, whereby the material's energy level was tuned and better matched with the perovskite [118]. Yoshida and co-workers doped TiO_2 with Magnesium which improved conductivity, tuned the conduction band levels, and, thus, increased the V_{oc} value [119].

Chen and Yang synthesized Ni-doped ZnO nanorods [120]. They proved that tuning the length and diameter of the nanorods can improve transmittance properties and reduce parasitic losses. The PCE obtained using this technique was above 13%, whereas for the undoped ZnO was 10.37%. Metals like Mg, Ca, Cs, Ga, Al, Pb and Li have been studied as ZnO dopants. This is to reduce the charge recombination at the perovskite/ETM interface, inhibit the chemical reaction at the interface and improve charge transfer, conductivity and stability.

Tseng and co-workers doped ZnO with Al using a sputtering technique to fabricate a device with 17.16% efficiency [121]. This improved performance can be associated with several reasons, a) better energy band matching with perovskite layer, b) Al doping improved charge transfer, c) Reduced acidic character of ZnO film. Zheng and co-workers elementally doped I^- to ZnO to, resulting in a PCE of 18.2% [122]. The I^- doping promoted the crystal growth of ZnO, regulated a compact structure and reduced charge recombination at the perovskite/ETM interface. Mahmud and co-workers even doped ZnO with Li to reduce trap states in the material [123]. Using this modified ETM in a triple cation perovskite resulted in a PCE greater than 16%. The doping of Li accounts for the following: a) reduced current leakage, b) improved charge extraction, and c) reduced trap density on the ZnO surface.

Using alkali metals as dopants have been regarded as a perfect passivating layer with abilities to improve electron transfer. K-doped ZnO improved the PCE of its ZnO counterpart

from 16.10% to 19.90% [124]. Al-doped ZnO was reported to reduce charge recombination and improve V_{oc} and FF values. Seok and co-workers used La-doped $BaSnO_3$ to fabricate a device with a PCE greater than 20% and excellent stability [125]. Sr-doped $BaSnO_3$ is another recently used strategy where the bandgap was further widened, enhancing V_{oc} and FF values [126]. Alkali metals doped ZnO is an effective strategy to generate more charge transfer pathways. Azmi and co-workers conducted a comparative analysis using Li, Na and K-doped ZnO [127]. The best performance was obtained from the K-based device with reduced hysteresis due to its superior passivation ability and trait to reduce charge recombination rates. The devices also possessed superior stability to air storage, where more than 90% of its initial PCE was retained. Al-doped ZnO is another helpful technique. An Al ion having a smaller radius can easily fit in the ZnO crystal lattice. Wu and co-workers used the same technique to produce Al-doped ZnO (AZO) ETM with improved conductivity, higher transmittance in the visible region, modified energy band levels and greater device efficiency (17.6%) [128]. AZO is exceptionally compatible with the perovskite layer, which also accounts for reduced recombination and increases device efficiency. Indium (In)-doped ZnO nanofibers were prepared where devices with no hysteresis and a device PCE greater than 17% were fabricated. In-doped ZnO produced high porosity and crystallinity films, which is responsible for favourable performance. While fabricating a ZnO-based device, a polyethyleneimine (PEI) interlayer is incorporated to inhibit smooth and stable deposition of the perovskite film. This further ensures less observed hysteresis and longer stability characteristics [129].

Heo and co-workers showed how doping Li-TFSI into TiO_2 to produce Li-doped TiO_2 can tune properties like mobility, conductivity, film quality and no hysteresis, with a PCE greater than 17% [130]. The elimination of hysteresis was attributed to the rapid charge transfer and separation by Li doping. The doping of TiO_2 with Li also shifted the conduction band, which increased the driving force and transportation of charges. Giordano and co-workers used a similar strategy with a thin layer of TiO_2 [131]. In this method, a mixed cation perovskite was used, and the device was fabricated inside a glove box to improve the PCE from 17% to 19.3%. The improvement in device efficiency is partly due to the reduced number of trap states. The reduction is because of the transitioning of Ti^{4+} to $Ti^{3+,}$ which modified the device layer to show improved performance.

SnO_2 as an ETM also requires a high temperature up to a certain extent to produce crystalline and pristine films. Dong and co-workers could bring this temperature limitation to 80 ^oC by using refluxes of H_2O and O_2 gases [132]. Moreover, using Aluminium as a dopant for SnO_2 can increase electrical conductivity and help improve device efficiency. Y-doped SnO_2 nanosheets are a technique that has been used previously. It was observed that the formed nanosheets were extremely homogeneous and improved contact between the ETM and perovskite. Nb-doped SnO_2 synthesized via the CBD process showed reduced series resistance values with a high J_{sc}, V_{oc}, FF and PCE value of 20.47% [133]. A device was fabricated whereby Zn^+ doping was carried out for Nb_2O_5 through a solution-processable combustion method to yield a PCE of 17.70% [134]. The device retained nearly 80% of its PCE after 20 days of air exposure. Tsvetkov and co-workers tuned the energy band alignment of $SrTiO_3$ by doping it with Nb, which resulted in a downward shift of the conduction band. Thus, resulting in a PCE of 20.2% [135].

Chen and co-workers used a new configuration where ZnS was deposited on ZnO to improve device stability (Fig. 7) [136]. The ZnS coordinated with Pb ions to form a Zn-S-Pb arrangement which reduced the acidic nature of ZnO.

Park and co-workers depicted how doping of Li in SnO_2 produces much more favourable results [5]. The energy band alignment is shifted to better suit the electrodes and perovskite layer (Fig. 8). There is improved electron injection and charge separation observed. The device produced using the SnO_2 ETM was extraordinarily stable and applicable for flexible substrates.

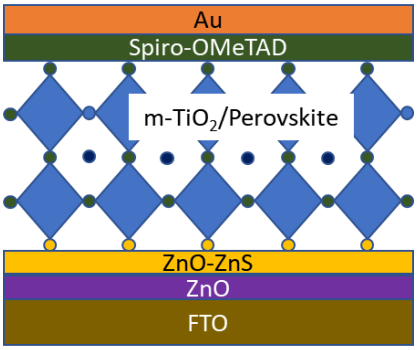

Fig. 7. Schematic Illustration of a Bilayer ZnO/ZnS Configuration

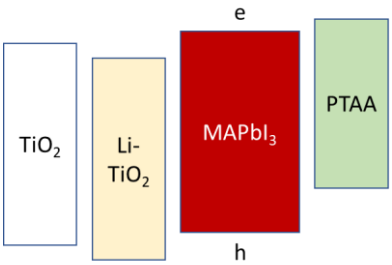

Fig. 8. Energy Band Alignment of Li-doped TiO_2

Surface Modification

This method is considered an alternative to doping and suitable treatment to remove defects. Chloride treatment, UV-Ozone (UVO), functional layer modification, exposure and comprehensive bandgap MO coating are some commonly incorporated methods.

Chloride treatment is used to treat MO films with $TiCl_4$ or KCl. Segawa and co-workers used a chloride treatment with $TiCl_4$ on TiO_2 [137]. It was observed that there is a notable increase in V_{oc}. A similar phenomenon can be observed in SnO_2, where there is not only an increase in a photovoltaic output parameter, the produced films are homogenous, smooth and dense [138]. Chloride treatment has been studied to reduce trap density and surface-related defects and facilitate smoother charge transport. TiO_2 and Cl (TiO_2-Cl) incorporated devices depicted improved stability characteristics, more substantial adhering effects between the perovskite and ETM and reduced charge recombination rates. Hao and co-workers showed how using KCl as an interlayer between the ETM and perovskite can passivate defects and improve stability.

UVO treatment is often used in producing pinhole-free, uniform and wettable surface films with reduced defects and traps. The films obtained are incredibly smooth and have tuned electrical properties to a certain extent [139]. It was reported that UVO-treated SnO_2-based devices improved the device efficiency from 11.49 to 16.21%. This shows that UVO treatment can vary the optoelectronic properties of the treated film.

Functional layer modification is another considered method to reduce charge recombination, passivate surface defects and traps, and improve device performance. Typically, this method is utilized at the interfaces of the device. Snaith and co-workers developed a TiO_2 ETM with a compact layer of C_{60} which passivated traps and improved charge traps [140]. This increased the PCE by greater than 17% with reduced hysteresis. Yang and co-workers used a functional fullerene layer along with SnO_2, reducing charge traps and improving interfacial charge transfer [141].

Coating of wide bandgap MO is a viable strategy that helps reduce interfacial charge recombination and improve device performance. A thin layer of MgO was used between the perovskite/ETM interface, which reduced charge recombination and improved V_{oc} and FF values [142]. Al_2O_3 and Y_2O_3 ultrathin layers have also been used as a coating layer aimed at passivating surface defects, reducing recombination, facilitating interfacial charge transfer and thus improving device performance [143].

Zhang and co-workers used 1-ethyl-3-methylimidazolium hexafluorophosphate as an interlayer between the ZnO and perovskite layer which tuned the energy band alignment [144]. Polymers like PVP can improve perovskite stability by eliminating -OH radical formation and also promoting better adhesion and wettability. Zuo and co-workers used 3-amino propanoic acid as a surface modifier to improve crystallinity [145]. Liu and co-workers used a coupled method of self-assembled monolayer (SAM) and self-form solvent annealing (SFSA) [146]. The SFSA method promoted crystal growth to produce more prominent grains and reduce grain boundaries. SAM passivated the surface defects and is an effective method to eliminate hysteresis.

Yang and co-workers developed a TiO_2-based polyethyleneimine (PEI) device to produce a PCE greater than 19% [147]. The device was further improved by doping it with Yttrium as it improved the mobility of charge carriers and reduced interface charge recombination. Cojocaru and co-workers used a post-treatment method with $TiCl_4$ and UVO treatment to support perovskite growth [148]. The device yielded 16.9% efficiency. It was observed that treatment with $TiCl_4$ increased hydrophilicity and wettability. The treatment with UVO removed impurities and contaminants. Liu and co-workers developed a low-temperature synthesis process of TiO_2 whereby $TiCl_4$ treatment was done at varying concentrations to produce a uniform and pinhole-free film [149]. The devices fabricated through this method showed improved V_{oc} values and a device efficiency of 16.4%.

MO-Matrix Composites

Creating a hybrid composite matrix is regarded as improving performance and stability. This method incorporates a material such as noble metals, carbon materials, organic materials, etc., into the MO.

Au-based TiO_2 has been known to improve light absorption capabilities and reduce charge recombination [150]. These effects have contributed to the increase in J_{sc} and FF values. Ag-based TiO_2 contributes to light absorption in the more extended wavelength region. However, it is essential to note that there is an optimum loading level of Ag which cannot be surpassed. SnO_2 with Graphene QDs have produced more homogeneous films, improved energy band alignment and reduced charge transfer resistance [151]. Carbon-based materials like Reduced Graphene Oxide (RGO) and Carbon dots with MO have known for their retarding charge recombination ability and enhancing photovoltaic performance. Wang and co-workers developed Tungsten-modified Niobium Oxides with an annealing temperature of 120 ^{o}C [152]. The fabricated device showed a PCE of 15.65% on Polyethylene naphthalate (PEN) substrates with better electron transport properties.

Using polymers in MO ETMs is also a helpful strategy where the polymers interact with the ETM to improve device efficiency and stability. Liu and co-workers used EDTA-based SnO_2 nanoparticles ETM [153]. The resulting perovskite film formed was smooth, with larger grain sizes and higher crystallinity. Moreover, it was reported that using EDTA increased the charge transfer and reduced charge accumulation at the interface, suppressing the hysteresis effect. Polyethylene Glycol (PEG)-based SnO_2 produced high wettability and dense films.

Core-shell MO structures are another viable strategy combining the core and shell MO advantages. Zhang and co-workers used a core-shell arrangement of TiO_2-$BaTiO_3$ [154]. The $BaTiO_3$ shell reduced recombination sites and minimized TiO_2 aggregation. Moreover, this core-shell arrangement also promoted the reaction between PbI_2 and MAI to form a smoother and improved perovskite film quality with a PCE greater than 13%. Wang and co-workers used ZnO

nanorods with a ZnSe successive layer to form a device with 27% improved PCE [155]. The modification of ZnSe improved the stability of the device. Li and co-workers used a ZnO-SnO_2 core-shell arrangement synthesized through a solvothermal method [156]. The SnO_2 shell was responsible for alignment well with the perovskite and electrode layer. The ZnO core was responsible for high electron mobility to obtain a PCE greater than 14%.

Using nanocomposites of different MO in a lattice of a base MO can combine the benefits of both materials to form a superior ETM. Tian and co-workers used this strategy to develop a ZnO-SnO_2 ETM [157]. The resulting film showed combined benefits of both the metal oxides with excellent charge transfer, extraction and stability properties. One can also conclude that blending various compatible MOs into a base MO is a valuable strategy for tuning and obtaining fruitful results. Similarly, SnO2-TiO2 and ZnO-Zn2SnO4 nanocomposites have shown reduced charge recombination rates, thus improving device performance.

Bilayer Engineering

This method is known to optimize MO ETMs to their full potential. An organic/inorganic bilayer framework is commonly used due to its favourable properties and universal usage in different PSC architectures. Yan and co-workers developed SnO_2/PCBM, where the usage of fullerene can actively passivate surface defects and minimize grain boundaries to promote electron transfer [158] actively. A study showed that using C_{60} in an inverted configuration can tune the energy band alignment of ZnO to suit the perovskite better [159]. Chen and co-workers used a PCBM/CeO_x approach where the bilayer was useful for charge extraction, a shielding layer from the ambient environment and retard metal diffusion [160].

Okamoto and co-workers used a double-layer ETM to form $BaTiO_3$/TiO_2 with a PCE of 12.4% [161]. The $BaTiO_3$/TiO_2 bilayer improved the perovskite layer's crystallisation, producing larger grain sizes, and reducing grain boundaries and charge recombination. Xu and co-workers developed a bilayer system using ZnO nanorods and a PCBM layer to yield a PCE of 11.67% [162]. The PCBM layer in this configuration increased the roughness of the ZnO layer to increase the perovskite loading. Chandrashekar and co-workers used a Nitrogen-doped graphene/ZnO bilayer system to produce a PCE greater than 16% [163]. This bilayer system showed how perovskite surface coverage, wettability and crystallinity, can be increased for improved device performance.

Apostolopoulou and co-workers synthesized a TiO_x/In_2O_3 bilayer. In this case, the In_2O_3 energy bands match well with the perovskite, which helps in charge transfer [164]. Moreover, the In_2O_3 layer also passivates the TiO_2 surface defects. Similarly, Chen and co-workers developed a similar bilayer. However, they optimized it to form a pinhole layer with improved hole-blocking capacities [165]. Garcia and co-workers combined ZnO and TiO_2 [166]. Here, the ZnO surface defects were minimized by the TiO_2 modification and this improved charge transfer greatly. You and co-workers prepared a TiO_2/WO_3 bilayer to yield a PCE greater than 20% [167]. Wang and co-workers developed a bilayer using amorphous WO_x and SnO_2 to achieve a PCE of 20.52% [168]. Tai and co-workers used a modified layer of ZnO along with an ultrathin film of ZSO [169]. The ZSO layer prevented directed degradation of the perovskite layer due to ZnO.

Moreover, ZSO passivated surface defects of ZnO to yield better charge transfer and extraction with a PCE of 18.3%. Ke and co-workers used a TiO_2/ZnS bilayer which showed reduced charge recombination and improved charge transfer [170]. Chavan and co-workers developed a ZnS buffer layer for TiO_2 [171]. Here the role of the buffer layer is to retard interfacial charge recombination, thus yielding better PCE levels than its counterparts. Ito and co-workers used the Sb_2S_3 interlayer between TiO_2 and the perovskite layer to improve the PCE from 4.82% to 5.03%. The interlayer reduced ion migration, increased the blocking effect, and improved the device stability.

Mahmoudi and co-workers used mesoporous Al_2O_3 and graphene to get a champion PCE of 20.6% and superior stability properties (Fig. 9) [172]. This bilayer could reduce the shunting

pathways and trap states on the surface. Cao and co-workers used a ZnO layer covered with MgO. They protonated ethanolamine (EA) to obtain a PCE greater than 21% and no hysteresis [173]. Fang and co-workers used a CeO_x layer modified with PCBM to obtain high mobility and a chemically stable structure [174]. This arrangement also creates a natural shield of extrinsic and intrinsic stability factors. Xing and co-workers also used a PCBM/CeO_x bilayer with a PCE of 17.35% [175]. The shunt resistance (R_{sh}) and charge transfer resistance (R_{ct}) indicate that the bilayer and perovskite have a more vital ohmic contact.

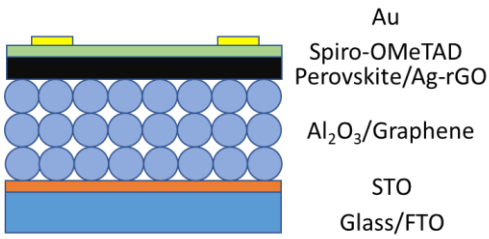

Fig. 9. Schematic Representation of a Graphene-Al_2O_3 Device

Wang and co-workers used a sol-gel method to synthesize CeO_x ETM films at 150 ^oC [176]. This film was then optimized by coupling it with PCBM. The resultant device showed excellent stability properties and a PCE of 17.04%. Meng and co-workers used a TiO_2/ZnO bilayer for planar PSCs [177]. As mentioned previously, the advantages of ZnO and TiO_2 were cumulated in this ETM to improve the device efficiency from 13.2 to 17.2%.

Energy Band Engineering

In a PSC device, its materials must have suitable energy band alignment. In doing so, there is efficient transport of charges, electron injection and appropriate charge collection at the electrodes. The transport, injection and collection of these charges are heavily dependent on the interfacial properties of materials, especially the ETM/perovskite and HTM/perovskite interface. A device's PCE is determined and optimized mainly by two stability factors: a) degradation of perovskite to extrinsic factors and b) lack of material compatibility, which impacts device structure.

Using insulated oxides which also behave as effective ETMs, is a suitable strategy. MOs like Al_2O_3, ZrO_2 and SiO_2 have improved device stability and properties [178-180]. Alumina is used as a growth mechanism layer for perovskite. Alumina has no oxygen defects, and its porous nature and semiconductor framework provide adequate stability and charge carrier features to replace the mesoporous TiO_2 ETM layer [181]. Insulating oxides behave as a scaffold layer as they have a higher conduction band maximum which eases the transport of electrons from the perovskite active layer to the electrode. Moreover, since the photoexcited electrons remain in the perovskite layer, it results in high V_{oc} values.

Wang and co-workers studied how treating the perovskite layer with alumina improves device stability and shows a stable performance [182]. Snaith and co-workers showed how Al_2O_3 behaves as a growth site and a possible ETM candidate to replace TiO_2 with exceptional stability of 1000 h under continuous stability [183]. Durrant and co-workers showed how Al_2O_3 could behave as a passivating layer [184]. It also acts as a diffusion barrier to the lead and metal electrode ions, which reduces trap density and improves crystal structure for better device performance.

Stability and Large Area Devices

The discussion shows that perovskite degradation is impacted by factors like moisture, heat, light, oxygen and ion migration. Zhao and co-workers eliminated the issue of thermal stability by doping ZnO with Al treated at 100 ˚C [185]. The resulting device depicted superior thermal stability properties due to the favourable reaction between the perovskite and ETM. Hou and co-workers used a PCBM layer on Haematite, resulting in better stability, where 95% of its initial PCE was retained after 45 days of dark storage [186]. Tavakoli and co-workers used a graphene monolayer between the ZnO and perovskite interface [187]. Such a modification prevented perovskite degradation evens at high temperatures. Moreover, the perovskite film was then passivated with PFPA. Through this PFPA and graphene modification, the device retained 93% of its initial PCE after 300 h of continuous light soaking.

Si and co-workers used an ultrathin layer of Al_2O_3 as an insulating layer between the ZnO and perovskite layer [188]. This restricted the interaction between ZnO, and the perovskite and Al_2O_3 protected the device from degradation. Brinkmann and co-workers used a similar strategy wherein the AZO/SnO_2 bilayer structure was used to create an extrinsic barrier and prevent perovskite decomposition [189]. Meng and co-workers used CeO_x/ZnO bilayer to produce a structure with improved UV, moisture, chemical and thermal stability [190]. This way, the device retained 90% of its initial PCE after 600 h of humid environment exposure. CeO_x is known to passivate ZnO defects and is a stable barrier against environmental factors. The improved thermal stability can be associated with the modified ZnO layer.

Large-scale device fabrication is essential for the commercialization of this technology. Currently, only TiO_2 and SnO_2-based MO devices have been proven effective (Fig. 10). Han and co-workers used an electrostatic self-assembly approach where large-scale SnO_2-based PSCs were fabricated [191]. The device efficiencies were 14% and 15.3% for 25 and 100 cm^2 active area devices, respectively. Hwang and co-workers fabricated a printable PSC using the slot-die coating method where P3HT-doped ZnO was used [192]. Since the method used is a hot slot die coating method, it promoted the reaction between MAI and PbI_2, resulting in better perovskite films.

Li and co-workers also used an inkjet approach to obtain reduced grain boundaries and increased grain sizes [193]. The device area was 2.02 $cm^{2,}$ with a PCE of 17.74%. The high device efficiency can be attributed to the improved device morphology. More recently, Liu and co-workers fabricated a large area PSC using Cs-based perovskite, NiO_x HTM and Nb_2O_5 as the ETM to obtain a PCE of 11.2% [194]. Moreover, the device showed excellent thermal stability. The improved device performance can be related to the reduced trap density and higher charge transfer.

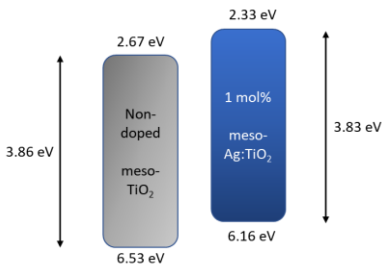

Fig. 10. Schematic Energy Band Diagram of Doped and Non-Doped Meso-TiO_2

Strategy to find Appropriate MO ETMs

Firstly, its properties must be estimated, calculated and studied to predict a particular material. This is done using a computational Density Functional Theory (DFT) method. Using DFT studies, we can study the electronic properties of a particular material and how well its properties align with being an ideal ETM [195]. However, it is essential to note that predictions made using computer-based methods need to be validated or agreed upon using certain assumptions.

Secondly, once favourable results are obtained through DFT analysis, the lab analysis is what follows. The material's properties, like energy bandgap, Fermi levels, mobility value, transmittance and more, are studied through practical and on-ground testing. As evident as it might seem, it is necessary that all the required conditions for MO ETMs are satisfied [196]. Even if one of these conditions is not satisfied, the material is excluded, and newer materials are developed.

Lastly, studying the case of wide bandgap MOs, the few important factors in synthesizing such ETMs would be the quality of the film produced, processing conditions, fabrication costs and processing method [3]. It is necessary to highlight that there needs to be an intersection between processing conditions, film quality, device stability and efficiency in obtaining a commercial and high-efficiency PSC. This underlying process of MO ETMs includes several complicated processes in the backend: a) synthesizing colloidal nanoparticles, b) using an appropriate washing process, and c) depositing the colloidal nanoparticles on the substrate.

Conclusion

The stability and compatibility of various materials in a PSC can be improved by using a MO as the HTM and ETM. However, this is not favourable as using MOs in both the charge transport materials requires temperatures greater than 100 ^{o}C. This is not appropriate as high temperatures can promote degradation of the perovskite layer. Moreover, due to their reduced processing temperatures, researchers prefer using fullerene-based molecules as a countercharge transport material. Spin-coating of a dispersed solution of nanomaterials or MO precursor solution supports the motive of low-temperature processing and paves the way for a more fantastic synthesis process.

This review concludes that the significant ETM candidates (but not limited to) are TiO_2, SnO_2 and ZnO. Irrespective of the ETM material, the current research focuses on how one can reduce trap states, tackle oxygen defects and promote the smoother transfer of charges even across interfaces. As evident as it is, MO ETMs are highly stable with better electrical and optical properties. However, the need to identify a suitable production process, economically viable, suitable performance and stability properties is the current challenge that remains.

These preparation methods should be low-cost and have low temperatures, which justifies the need for commercialization, especially on flexible substrates. The flexibility and compatibility whilst considering various synthesis processes need to be carefully evaluated. Interfacial engineering is a valuable strategy that modulates the interface properties and passivates surface defects to enhance device stability and efficiency.

The optimal processing method or material does not necessarily depend on certain factors. However, before fabricating a MO-based device, it is suggested to consider the processing conditions, fabrication processes, cost and predicted efficiency values. Only when a suitable balance between efficiency and stability is observed is the device suggested for commercialization. A proposed method to reduce voltage loss is to deal significantly with the perovskite/ETM interface.

Although there have been significant developments in the field of low-temperature MO PSCs, further research and exploration still need to be conducted to produce high-efficiency

devices. Before a MO ETM is used in a device, one should consider the following factors, a) economic solution processibility, b) energy band alignments, c) electron mobility values, and d) stability properties. In the case of flexible PSCs, the brittle nature of MO ETMs makes it slightly more difficult in this application. Thus, researchers need to examine more blending strategies that tune the MO properties, making them more suitable for flexible device applications.

The next research step needs to also focus on using more unconventional MO materials in low-dimensional, mixed and hybrid perovskite devices to produce large-area, flexible and commercial devices. Moreover, one must also look into producing these devices through a roll-to-roll process so that commercialization is easier and the properties can be expanded beyond PSCs to other flexible and optoelectronic devices.

With theoretical and experimental calculations, one should look into a method that can maximize output levels and material properties whilst regulating device processing costs and time. Studying the perovskite/ETM interface is a separate and vital branch of study that can be dealt with by using various chemical or physical methods. Another aspect of MO ETMs that one can consider is to regulate and controllably modify the material's crystallinity, morphology and composition. Even considering fabricating large-area PSCs can put a realistic demand on how these technologies can be fabricated with more favourable properties.

References

[1] Singh, M., Chu, C., Ng, A, *Perspective on Predominant Metal Oxide Charge Transporting Materials for High-Performance Perovskite Solar Cells*, **Frontiers In Materials, 8**, 2021, p. 655207. DOI: 10.3389/fmats.2021.655207.

[2] Song, JX., Yin, XX., Li, ZF. et al., *Low-temperature-processed metal oxide electron transport layers for efficient planar perovskite solar cells*, **Rare Met., 40**, 2021, pp. 2730–2746. DOI: 10.1007/s12598-020-01676-y.

[3] S. S. Shin, S. J. Lee, and S. I. Seok, *Exploring wide bandgap metal oxides for perovskite solar cells*, **APL Materials, 7**, 2019, p. 022401. DOI: 10.1063/1.5055607.

[4] Cao, Z., Li, C., Deng, X., Wang, S., Yuan, Y., & Chen, Y. et al. *Metal oxide alternatives for efficient electron transport in perovskite solar cells: beyond TiO2 and SnO2*. **Journal Of Materials Chemistry A, 8(38),** 2020, 19768-19787. DOI: 10.1039/d0ta07282f.

[5] Zhou, Y., Li, X., Lin, H., To *Be Higher and Stronger—Metal Oxide Electron Transport Materials for Perovskite Solar Cells*, **Small**, 16, 2020, p. 1902579. DOI: 10.1002/smll.201902579.

[6] Lee MM, Teuscher J, Miyasaka T, Murakami TN, Snaith HJ. *Efficient hybrid solar cells based on meso-superstructured organometal halide perovskites*, **Science**, **338(6107)**, 2012, pp. 643-647, DOI:10.1126/science.1228604.

[7] Mei A, Li X, Liu L, et al. *A hole-conductor-free, fully printable mesoscopic perovskite solar cell with high stability*, **Science**, 345(6194), 2014, pp. 295-298. DOI: 10.1126/science.1254763

[8] Dae-Yong S., Jeong-Hyeok I., Hui-Seon K., Nam-Gyu P., *11% Efficient Perovskite Solar Cell Based on ZnO Nanorods: An Effective Charge Collection System*, **The Journal of Physical Chemistry C, 118(30)**, 2014, pp. 16567-16573. DOI: 10.1021/jp412407j.

[9] Roose, B., Baena, J., Gödel, K., Graetzel, M., Hagfeldt, A., Steiner, U., & Abate, A. *Mesoporous SnO2 electron selective contact enables UV-stable perovskite solar cells*, **Nano Energy**, **30**, 2016, pp. 517-522. DOI: 10.1016/j.nanoen.2016.10.055.

[10] Zhou, H., Chen, Q., Li, G., Luo, S., Song, T.B., Duan, H.S., Hong, Z., You, J., Liu, Y. and Yang, Y., *Interface Engineering of Highly Efficient Perovskite Solar Cells*, **Science**, **345**, 2014, pp. 542-546. DOI: 10.1126/science.1254050.

[11] Saliba, M., Matsui, T., Seo, J., Domanski, K., Correa-Baena, J., & Nazeeruddin, M. et al. *Cesium-containing triple cation perovskite solar cells: improved stability, reproducibility and high efficiency*. **Energy &Amp; Environmental Science**, **9(6)**, 2016, pp. 1989-1997. DOI: 10.1039/c5ee03874j.

[12] Jeon, N., Na, H., Jung, E., Yang, T., Lee, Y., & Kim, G. et al. *A fluorene-terminated hole-transporting material for highly efficient and stable perovskite solar cells*. **Nature Energy**, **3(8)**, 2018, pp. 682-689. DOI: 10.1038/s41560-018-0200-6.

[13] Jeon, N.J., Noh, J.H., Yang, W.S., Kim, Y.C., Ryu, S., Seo, J. and Seok, S.I. *Compositional Engineering of Perovskite Materials for High-Performance Solar Cells*, **Nature**, **517**, 2015 pp. 476-480. DOI: 10.1038/nature14133.

[14] Valadi, K., Gharibi, S., Taheri-Ledari, R. et al. *Metal oxide electron transport materials for perovskite solar cells: a review*. **Environ Chem Lett., 19**, 2185–2207, 2021, DOI: 10.1007/s10311-020-01171-x

[15] Guerrero, A., Juarez-Perez, E., Bisquert, J., Mora-Sero, I., & Garcia-Belmonte, G., *Electrical field profile and doping in planar lead halide perovskite solar cells*, **Applied Physics Letters**, **105(13)**, 2014, p. 133902. DOI: 10.1063/1.4896779.

[16] Laban, W., & Etgar, L. *Depleted hole conductor-free lead halide iodide heterojunction solar cells*, **Energy &Amp; Environmental Science**, **6(11)**, 2013, p. 3249. DOI: 10.1039/c3ee42282h.

[17] Shin, S., Lee, S., & Seok, S., *Exploring wide bandgap metal oxides for perovskite solar cells*, **APL Materials**, **7(2)**, 2019, p. 022401. DOI: 10.1063/1.5055607.

[18] Fan Z., Wei M., Haizhong G., Yicheng Z., Xinyan S., Kuijuan J., He T., Qing Z., Dapeng Y., Xinghua L., Gang L., Sheng M., *Interfacial Oxygen Vacancies as a Potential Cause of Hysteresis in Perovskite Solar Cells*, **Chemistry of Materials, 28(3)**, 2016, pp. 802-812. DOI: 10.1021/acs.chemmater.5b04019.

[19] Tan H., Jain A., Voznyy O., et al. *Efficient and stable solution-processed planar perovskite solar cells via contact passivation*, **Science, 355(6326),** 2017, pp. 722-726. DOI: 10.1126/science.aai9081

[20] Thomas, A. *A Review on Antimony-based Perovskite Solar Cells*, **Equilibrium Journal of Chemical Engineering**, **6(2)**, 2022, pp. 75-91. DOI: 10.20961/equilibrium.v6i2.64322.

[21] Yaoguang R., Yue M., Wenxian J., Da L., Anyi M., Yue H., Hongwei H. *Toward Industrial-Scale Production of Perovskite Solar Cells: Screen Printing, Slot-Die Coating, and Emerging Techniques*, **The Journal of Physical Chemistry Letters, 9(10)**, 2018, pp. 2707-2713. DOI: 10.1021/acs.jpclett.8b00912

[22] Jiang, Q., Chu, Z., Wang, P., Yang, X., Liu, H., Wang, Y., et al. *Planarstructure perovskite solar cells with efficiency beyond 21%*, **Adv. Mater. 29,** 2017, p. 1703852. DOI: 10.1002/adma.201703852.

[23] Cao, J., Wu, B., Chen, R., Wu, Y., Hui, Y., Mao, B. W., et al. *Efficient, hysteresis-Free, and stable perovskite solar cells with ZnO as electron-transport layer: effect of surface passivation*, **Adv. Mater., 30**, 2018, p. 1705596. DOI: 10.1002/adma.201705596.

[24] Elseman, A. M., Xu, C., Yao, Y., Elisabeth, M., Niu, L., Malavasi, L., et al. *Electron transport materials: evolution and case study for high-efficiency perovskite solar cells*, **Solar RRL, 4,** 2020, p. 2000136. DOI: 10.1002/solr.202000136.

[25] Zhang, P., Wu, J., Zhang, T., Wang, Y., Liu, D., Chen, H., Ji, L., Liu, C., Ahmad, W., Chen, Z. D., Li, S., *Perovskite Solar Cells with ZnO Electron-Transporting Materials*. **Adv. Mater.**, 30, 2018, p. 1703737. DOI: 10.1002/adma.201703737

[26] Miikkulainen, V., Leskelä, M., Ritala, M., & Puurunen, R., *Crystallinity of inorganic films grown by atomic layer deposition: Overview and general trends*, **Journal Of Applied Physics**, **113(2)**, 2013, p. 021301. DOI: 10.1063/1.4757907.

[27] P. K. Nair, M. T. S. Nair, V. M. Garcı´a, O. L. Arenas, A. C. Y. Peña, I. T. Ayala, O. Gomezdaza, A. Sánchez, J. Campos, H. Hu, R. Suárez, M. E. Rincón, *Sol. Energy Mater. Sol*. **Cells**, **52**, 1998, p. 313.

[28] Bingqiang C., Weiping C., *From ZnO Nanorods to Nanoplates: Chemical Bath Deposition Growth and Surface-Related Emissions*, **The Journal of Physical Chemistry C**, **112(3)**, 2008, pp. 680-685. DOI: 10.1021/jp076870l.

[29] Ibrahem, M. A., Huang, W.-C., Lan, T.-W., Boopathi, K. M., Hsiao, Y.-C., Chen, C.-H., et al. *Controlled mechanical cleavage of bulk niobium diselenide to nanoscaled sheet, rod, and particle structures for Pt-free dye-sensitized solar cells*, **J. Mater. Chem. A, 2**, 2014, pp. 11382–11390. DOI: 10.1039/C4TA01881H.

[30] Ding, J., Abbas, S. A., Hanmandlu, C., Lin, L., Lai, C.-S., Wang, P.-C., et al. *Facile synthesis of carbon/MoO3 nanocomposites as stable battery anodes*, **J. Power Sources**, 348, 2017, pp. 270–280. DOI: 10.1016/j.jpowsour.2017.03.007.

[31] Mali, S., Shim, C., & Hong, C., *Highly stable and efficient solid-state solar cells based on methylammonium lead bromide (CH3NH3PbBr3) perovskite quantum dots*. **NPG Asia Materials, 7(8)**, 2015, p. e208-e208. DOI: 10.1038/am.2015.86.

[32] Wang, Y., Su, T., Tsai, H., Wei, T., & Chi, Y. *Spiro-Phenylpyrazole/Fluorene as Hole-Transporting Material for Perovskite Solar Cells*. **Scientific Reports**, **7(1)**, 2017. DOI: 10.1038/s41598-017-08187-4.

[33] Wang, Z., Zhang, D., Yang, G., & Yu, J. *Exceeding 19% efficiency for inverted perovskite solar cells used conventional organic small molecule TPD as hole transport layer*. **Applied Physics Letters**, **118(18)**, 2021, p. 183301. DOI: 10.1063/5.0050512.

[34] Yang, D., Yang, R., Zhang, J., Yang, Z., (Frank) Liu, S., & Li, C. *High efficiency flexible perovskite solar cells using superior low temperature TiO2*, **Energy &Amp; Environmental Science**, **8(11)**, 2015, pp. 3208-3214. DOI: 10.1039/c5ee02155c.

[35] Ma, J., Zheng, X., Lei, H., Ke, W., Chen, C., Chen, Z., Yang, G. and Fang, G. *Highly Efficient and Stable Planar Perovskite Solar Cells With Large-Scale Manufacture of E-Beam Evaporated SnO2 Toward Commercialization*. **Sol. RRL**, **1**, 2017, p. 1700118. DOI: 10.1002/solr.201700118.

[36] Wang, J., Meng, J., Li, Q., & Yang, J. *Single-layer cadmium chalcogenides: promising visible-light driven photocatalysts for water splitting*. **Physical Chemistry Chemical Physics**, **18(25)**, 2016, pp. 17029-17036. DOI: 10.1039/c6cp01001f.

[37] Lin, Y., Chen, B., Zhao, F., Zheng, X., Deng, Y., Shao, Y., Fang, Y., Bai, Y., Wang, C., Huang, J., *Matching Charge Extraction Contact for Wide-Bandgap Perovskite Solar Cells*, **Adv. Mater.**, **29**, 2017, p. 1700607. DOI: 10.1002/adma.201700607.

[38] Saliba, M., Matsui, T., Seo, J. Y., Domanski, K., Correa-Baena, J. P., Nazeeruddin, M. K., Zakeeruddin, S. M., Tress, W., Abate, A., Hagfeldt, A., & Grätzel, M., *Cesium-containing triple cation perovskite solar cells: improved stability, reproducibility and high efficiency*, **Energy & environmental science**, **9(6)**, 2016, pp. 1989–1997. DOI: 10.1039/c5ee03874j.

[39] Niu, G., Guo, X., & Wang, L. *Review of recent progress in chemical stability of perovskite solar cells*, **Journal of Materials Chemistry A**, **3(17)**, 2015, pp. 8970-8980. DOI: 10.1039/c4ta04994b.

[40] Thomas, A.S., *Charge Transport Materials, Bismuth and Copper-Based Perovskite Solar Cells: A Review*, **Future Energy, 1 (3),** 2022, pp. 19-43.

[41] Thomas, A.S., *Film Properties Using Metal Salts Washing for Perovskite Solar Cells*, **Preprints**, 2022, p. 2022070192, DOI: 10.20944/preprints202207.0192.v1.

[42] Jung, E. H., Jeon, N. J., Park, E. Y., Moon, C. S., Shin, T. J., Yang, T. Y., Noh, J. H., & Seo, J., *Efficient, stable and scalable perovskite solar cells using poly(3-hexylthiophene)*, **Nature**, **567(7749)**, 2019, pp. 511–515. DOI: 10.1038/s41586-019-1036-3.

[43] Docampo, P., Ball, J. M., Darwich, M., Eperon, G. E., & Snaith, H. J. *Efficient organometal trihalide perovskite planar-heterojunction solar cells on flexible polymer substrates*, **Nature communications**, **4**, 2013, p. 2761. DOI: 10.1038/ncomms3761.

[44] Conings, B., Baeten, L., Jacobs, T., Dera, R., D'Haen, J., Manca, J., & Boyen, H. *An easy-to-fabricate low-temperature TiO2 electron collection layer for high efficiency planar heterojunction perovskite solar cells*, **APL Materials**, **2(8)**, 2014, p. 081505. DOI: 10.1063/1.4890245.

[45] Kim, B., Kim, D., Lee, Y., Shin, H., Han, G., & Hong, J. et al. *Highly efficient and bending durable perovskite solar cells: toward a wearable power source*, **Energy &Amp; Environmental Science**, **8(3)**, 2015, pp. 916-921. DOI: 10.1039/c4ee02441a.

[46] Aswani Y., Leo-Philipp H., Peng G., Mohammad K.N., Michael G., *Nanocrystalline Rutile Electron Extraction Layer Enables Low-Temperature Solution Processed Perovskite Photovoltaics with 13.7% Efficiency*, **Nano Letters, 14(5)**, 2014, pp. 2591-2596. DOI: 10.1021/nl500399m.

[47] Chen, C., Cheng, Y., Dai, Q., Song, H. *Radio Frequency Magnetron Sputtering Deposition of TiO2 Thin Films and Their Perovskite Solar Cell Applications*. **Scientific reports**, **5**, 2015, p. 17684. DOI: 10.1038/srep17684.

[48] Zhu Y., Zhu Y., Deng K., Sun H., Gu B., Lu H., Cao F., Xiong J., Li L., *TiO2 phase junction electron transport layer boosts efficiency of planar perovskite solar cells*, **Adv Sci, 5(3)**, 2018, p. 1700614. DOI: 10.1002/advs.20170 0614.

[49] Ye X., Xinxin W., Zhuo C., Dieter W., Yingying W., Lijie S., Xiao M., Chunjie D., Wei L., Shuai G., Ruibin L., *Polarization-Sensitive Self-Powered Type-II GeSe/MoS2 van der Waals Heterojunction Photodetector*, **ACS Applied Materials & Interfaces**, **12(13)**, 2020, pp. 15406-15413. DOI: 10.1021/acsami.0c01405.

[50] Song, J., Zheng, E., Bian, J., Wang, X., Tian, W., Sanehira, Y., & Miyasaka, T. *Low-temperature SnO2-based electron selective contact for efficient and stable perovskite solar cells*, **Journal of Materials Chemistry A**, **3(20)**, 2015, pp. 10837-10844. DOI: 10.1039/c5ta01207d.

[51] Li, Y., Zhu, J., Huang, Y., Liu, F., Lv, M., & Chen, S. et al. *Mesoporous SnO2nanoparticle films as electron-transporting material in perovskite solar cells*. **RSC Advances**, **5(36)**, 2015, pp. 28424-28429. DOI: 10.1039/c5ra01540e.

[52] Ke, W., Fang, G., Liu, Q., Xiong, L., Qin, P., Tao, H., Wang, J., Lei, H., Li, B., Wan, J., Yang, G., Yan, Y. *Low-temperature solution-processed tin oxide as an alternative electron transporting layer for efficient perovskite solar cells*, **Journal of the American Chemical Society**, **137(21)**, 2015, pp. 6730–6733. DOI: 10.1021/jacs.5b01994.

[53] Zhu, Z., Bai, Y., Liu, X., Chueh, C. C., Yang, S., Jen, A. K., *Enhanced Efficiency and Stability of Inverted Perovskite Solar Cells Using Highly Crystalline SnO2 Nanocrystals as the Robust Electron-Transporting Layer*, **Advanced materials (Deerfield Beach, Fla.)**, **28(30)**, 2016, pp. 6478–6484. DOI: 10.1002/adma.201600619.

[54] Ziheng Z., Xitao L., Lingling X., Bingkun C., Ting J., Jie C., Fa Z., Min W., Yafeng W., Hong Z., Fang Z., Yongtian W., *Phase control in the synthesis of cesium copper iodide compounds for their photoluminescence and radioluminescence study*, **Journal of Luminescence**, **241**, 2022, p. 118482. DOI: 10.1016/j.jlumin.2021.118482.

[55] Zhang, D., Wu, J., Cao, Y. *Cobalt-doped indium oxide/molybdenum disulfide ternary nanocomposite toward carbon monoxide gas sensing*, **Journal Of Alloys And Compounds**, **777**, 2019, pp. 443-453. DOI: 10.1016/j.jallcom.2018.10.365.

[56] Changlei W., Lei G., Dewei Z., Yue Y., Corey R.G., Zhaoning S., Rasha A. A., Jing C., Jianbo W., Xingzhong Z., Yanfa Y., *Water Vapor Treatment of Low-Temperature Deposited SnO2 Electron Selective Layers for Efficient Flexible Perovskite Solar Cells*, **ACS Energy Letters, 2(9)**, 2017, pp. 2118-2124. DOI: 10.1021/acsenergylett.7b00644.

[57] Weijun K., Guojia F., Qin L., Liangbin X., Pingli Q., Hong T., Jing W., Hongwei L., Borui L., Jiawei W., Guang Y., Yanfa Y., *Low-Temperature Solution-Processed Tin Oxide as an Alternative Electron Transporting Layer for Efficient Perovskite Solar Cells*, **Journal of the American Chemical Society, 137(21)**, 2015, pp. 6730-6733. DOI: 10.1021/jacs.5b01994.

[58] Chenxiao Z., Alexey B.T., Eugene A.G., Pengwan C., Hao W., Qi C., *Recent strategies to improve moisture stability in metal halide perovskites materials and devices*, **Journal of Energy Chemistry**, **65**, 2022, pp. 219-235. DOI: 10.1016/j.jechem.2021.05.035.

[59] Anand S.S., Nripan M., Subodh M., Shaibal K. S., *Novel Plasma-Assisted Low-Temperature-Processed SnO2 Thin Films for Efficient Flexible Perovskite Photovoltaics*, **ACS Energy Letters, 3(7)**, 2018, pp. 1482-1491. DOI: 10.1021/acsenergylett.8b00692.

[60] Bu, T., Li, J., Zheng, F., Chen, W., Wen, X., Ku, Z., Peng, Y., Zhong, J., Cheng, Y. B., Huang, F., *Universal passivation strategy to slot-die printed SnO2 for hysteresis-free efficient flexible perovskite solar module*, **Nature communications**, **9(1)**, 2018, p. 4609. DOI: 10.1038/s41467-018-07099-9.

[61] Bi, D., Boschloo, G., Schwarzmüller, S., Yang, L., Johansson, E., & Hagfeldt, A. *Efficient and stable CH3NH3PbI3-sensitized ZnO nanorod array solid-state solar cells*. **Nanoscale**, **5(23)**, 2013, pp. 11686. DOI: 10.1039/c3nr01542d

[62] Liu, D., & Kelly, T. *Perovskite solar cells with a planar heterojunction structure prepared using room-temperature solution processing techniques*. **Nature Photonics**, **8(2)**, 2013, pp. 133-138. DOI: 10.1038/nphoton.2013.342.

[63] Wang, G., Long, S., Yu, Z., Zhang, M., Ye, T., & Li, Y. et al. *Improving resistance uniformity and endurance of resistive switching memory by accurately controlling the stress time of pulse program operation*, **Applied Physics Letters**, **106(9)**, 2015, p. 092103. DOI: 10.1063/1.4907604.

[64] You, J., Meng, L., Song, T. B., Guo, T. F., Yang, Y. M., Chang, W. H., Hong, Z., Chen, H., Zhou, H., Chen, Q., Liu, Y., De Marco, N., & Yang, Y. *Improved air stability of perovskite solar cells via solution-processed metal oxide transport layers*, **Nature nanotechnology**, **11(1)**, 2016, pp. 75–81. DOI: 10.1038/nnano.2015.230.

[65] Berger, P., & Kim, M. *Polymer solar cells: P3HT:PCBM and beyond*, **Journal Of Renewable And Sustainable Energy**, **10(1)**, 2018, p. 013508. DOI: 10.1063/1.5012992.

[66] Son D.Y., Im J.H., Kim H.S., Park N.G., *11% efficient perovskite solar cell based on ZnO nanorods: an effective charge collection system*. **J Phys Chem C**, **118(30),** 2014, pp. 16567–16573. DOI: 10.1021/jp412 407j.

[67] Ouyang, D., Huang, Z., Choy, W. C. H., *Adv. Funct. Mater.*, **29**, 2019, p. 1804660. DOI: 10.1002/adfm.201804660.

[68] Song, J., Hu, W., Wang, X., Chen, G., Tian, W., & Miyasaka, T. *HC(NH2)2PbI3as a thermally stable absorber for efficient ZnO-based perovskite solar cells*. **Journal Of Materials Chemistry A**, **4(21)**, 2016, pp. 8435-8443. DOI: 10.1039/c6ta01074a.

[69] Zhou, J., Meng, X., Zhang, X., Tao, X., Zhang, Z., & Hu, J. et al. *Low-temperature aqueous solution processed ZnO as an electron transporting layer for efficient perovskite solar cells*, **Materials Chemistry Frontiers**, **1(5)**, 2017, pp. 802-806. DOI: 10.1039/c6qm00248j.

[70] Kumar, M., Yantara, N., Dharani, S., Graetzel, M., Mhaisalkar, S., Boix, P., & Mathews, N., *Flexible, low-temperature, solution processed ZnO-based perovskite solid state solar cells*, **Chemical Communications**, **49(94)**, 2013, p. 11089. DOI: 10.1039/c3cc46534a.

[71] Ali Ahmad, S., Ashfaq, A., Akbar, M., Ikram, M., Khan, K., & Wang, F. et al. *Application of two-dimensional materials in perovskite solar cells: recent progress, challenges, and prospective solutions,* **Journal Of Materials Chemistry C**, **9(40)**, 2021, pp. 14065-14092. DOI: 10.1039/d1tc02407h.

[72] Wang B, Zhong S, Lee T-L, Fancey KS, Mi J. *Non-destructive testing and evaluation of composite materials/structures: A state-of-the-art review*, **Advances in Mechanical Engineering, 12(4)**, 2020. DOI:10.1177/1687814020913761.

[73] Hu, W., Liu, T., Yin, X., Liu, H., Zhao, X., & Luo, S. et al. *Hematite electron-transporting layers for environmentally stable planar perovskite solar cells with enhanced energy conversion and lower hysteresis,* **Journal Of Materials Chemistry A**, **5(4)**, 2017, pp. 1434-1441. DOI: 10.1039/c6ta09174a.

[74] Shin, S. S., Yang, W. S., Noh, J. H., Suk, J. H., Jeon, N. J., Park, J. H., Kim, J. S., Seong, W. M., & Seok, S. I., *High-performance flexible perovskite solar cells exploiting Zn2SnO4 prepared in solution below 100 °C,* **Nature communications**, **6**, 2015, p. 7410. DOI: 10.1038/ncomms8410.

[75] Nakazaki, J., & Segawa, H., *Evolution of organometal halide solar cells*, **Journal Of Photochemistry And Photobiology C: Photochemistry Reviews**, **35**, 2018, pp. 74-107. DOI: 10.1016/j.jphotochemrev.2018.02.002.

[76] Kyungeun J., Jeongwon L., Chan I., Junghwan D., Joosun K., Weon-Sik C., Man-Jong L., *Highly Efficient Amorphous Zn2SnO4 Electron-Selective Layers Yielding over 20% Efficiency in FAMAPbI3-Based Planar Solar Cells,* **ACS Energy Letters**, **3(10)**, 2018, pp. 2410-2417. DOI: 10.1021/acsenergylett.8b01501.

[77] Tavakoli, M., Tavakoli, R., Prochowicz, D., Yadav, P., Saliba, M., *Surface modification of a hole transporting layer for an efficient perovskite solar cell with an enhanced fill factor and stability,* **Molecular Systems Design &Amp; Engineering**, **3(5)**, 2018, pp. 717-722. DOI: 10.1039/c8me00036k.

[78] Lee Seul O., Dong Hoe K., Jin Ah L., Seong Sik S., Jin-Wook L., Ik Jae P., Min Jae K., Nam-Gyu P., Sung Gyu P., Kug Sun H., Jin Young K., *Zn2SnO4-Based Photoelectrodes for Organolead Halide Perovskite Solar Cells,* **The Journal of Physical Chemistry C, 118(40)**, 2014, pp. 22991-22994. DOI: 10.1021/jp509183k.

[79] Liu, X., Yang, Z., Chueh, C., Rajagopal, A., Williams, S., Sun, Y., Jen, A. *Improved efficiency and stability of Pb–Sn binary perovskite solar cells by Cs substitution,* **Journal Of Materials Chemistry A**, **4(46)**, 2016, pp. 17939-17945. DOI: 10.1039/c6ta07712a.

[80] Zhu, L., Shao, Z., Ye, J., Zhang, X., Pan, X., & Dai, S. *Mesoporous BaSnO3 layer based perovskite solar cells,* **Chemical Communications**, **52(5)**, 2016, pp. 970-973. DOI: 10.1039/c5cc08156d.

[81] Suresh Kumar, N., Chandra B.N.K. *A review on perovskite solar cells (PSCs), materials and applications,* **Journal of Materiomics**, **7(5)**, 2021, pp. 940-956. DOI: 10.1016/j.jmat.2021.04.002.

[82] Zhu, L., Ye, J., Zhang, X., Zheng, H., Liu, G., Pan, X., & Dai, S. *Performance enhancement of perovskite solar cells using a La-doped BaSnO3 electron transport layer,* **Journal Of Materials Chemistry A**, **5(7)**, 2017, pp. 3675-3682. DOI: 10.1039/c6ta09689a.

[83] Yantao W., Aleksandra B.D., Wei C., Fangzhou L., Rui C., Shien P.F., Alan M.C.N. Zhubing H., *Metal oxide charge transport layers in perovskite solar cells—optimising low temperature processing and improving the interfaces towards low temperature processed, efficient and stable devices,* **Journal of Physics: Energy**, **3(1)**, 2020, p. 012004. DOI 10.1088/2515-7655/abc73f.

[84] Shin, S. S., Yeom, E. J., Yang, W. S., Hur, S., Kim, M. G., Im, J., Seo, J., Noh, J. H., & Seok, S. I. *Colloidally prepared La-doped BaSnO3 electrodes for efficient, photostable perovskite solar cells,* **Science (New York, N.Y.)**, **356(6334)**, 2017, pp. 167–171. DOI: 10.1126/science.aam6620.

[85] Haoliang C., Yaru L., Guanyu Z., Ke Z., Zhong-Sheng W., *Pyridine-Terminated Conjugated Organic Molecules as an Interfacial Hole Transfer Bridge for NiOx-Based Perovskite Solar Cells*, **ACS Applied Materials & Interfaces**, **11(32)**, 2019, pp. 28960-28967. DOI: 10.1021/acsami.9b09530.

[86] Mahmood, K., Swain, B., Kirmani, A., & Amassian, A., *Highly efficient perovskite solar cells based on a nanostructured WO3–TiO2core–shell electron transporting material*, **Journal Of Materials Chemistry A**, **3(17)**, 2015, pp. 9051-9057. DOI: 10.1039/c4ta04883k.

[87] Feng, J., Zhu, X., Yang, Z., Zhang, X., Niu, J., Wang, Z., Zuo, S., Priya, S., Liu, S. (F.), Yang, D., *Record Efficiency Stable Flexible Perovskite Solar Cell Using Effective Additive Assistant Strategy*, **Adv. Mater., 30**, 2018, p. 1801418. DOI: 10.1002/adma.201801418.

[88] Ablikim, M., Achasov, M. N., Ai, X. C., Albayrak, O., Albrecht, M., Ambrose, D. J., Amoroso, A., An, F. F., An, Q., Bai, J. Z., Baldini Ferroli, R., Ban, Y., Bennett, D. W., Bennett, J. V., Bertani, M., Bettoni, D., Bian, J. M., Bianchi, F., Boger, E., Boyko, I., … BESIII Collaboration, *Determination of the Spin and Parity of the Z_{c}(3900)*. **Physical review letters**, **119(7)**, 2017, p. 072001. DOI: 10.1103/PhysRevLett.119.072001.

[89] Kogo, A., Ikegami, M., & Miyasaka, T. *A SnOx–brookite TiO2 bilayer electron collector for hysteresis-less high efficiency plastic perovskite solar cells fabricated at low process temperature*, **Chemical Communications**, **52(52)**, 2016, pp. 8119-8122. DOI: 10.1039/c6cc02589g.

[90] Zhu, X., Yang, D., Yang, R., Yang, B., Yang, Z., & Ren, X. et al., *Superior stability for perovskite solar cells with 20% efficiency using vacuum co-evaporation*, **Nanoscale**, **9(34)**, 2017, pp. 12316-12323. DOI: 10.1039/c7nr04501h.

[91] Feng, J., Yang, Z., Yang, D., Ren, X., Zhu, X., & Jin, Z. et al. *E-beam evaporated Nb2O5 as an effective electron transport layer for large flexible perovskite solar cells*, **Nano Energy**, **36**, 2017, pp. 1-8. DOI: 10.1016/j.nanoen.2017.04.010.

[92] Jiang, J., Wang, S., Jia, X., Fang, X., Zhang, S., & Zhang, J. et al. *Totally room-temperature solution-processing method for fabricating flexible perovskite solar cells using an Nb2O5–TiO2electron transport layer*, **RSC Advances**, **8(23)**, 2018, pp. 12823-12831. DOI: 10.1039/c8ra01571f.

[93] Juarez-Perez, E., Ono, L., Maeda, M., Jiang, Y., Hawash, Z., & Qi, Y., *Photodecomposition and thermal decomposition in methylammonium halide lead perovskites and inferred design principles to increase photovoltaic device stability*, **Journal Of Materials Chemistry A**, **6(20)**, 2018, pp. 9604-9612. DOI: 10.1039/c8ta03501f.

[94] Wang, X., Deng, L., Wang, L., Dai, S., Xing, Z., & Zhan, X. et al. *Cerium oxide standing out as an electron transport layer for efficient and stable perovskite solar cells processed at low temperature.* **Journal Of Materials Chemistry A**, **5(4)**, 2017, pp. 1706-1712. DOI: 10.1039/c6ta07541j.

[95] Hu, T., Xiao, S., Yang, H., Chen, L., Chen, Y. *Cerium oxide as an efficient electron extraction layer for p–i–n structured perovskite solar cells*, **Chemical Communications**, **54(5)**, 2018, pp. 471-474. DOI: 10.1039/c7cc08657a.

[96] Zhang, C., Arumugam, G., Liu, C., Hu, J., Yang, Y., Schropp, R., & Mai, Y. *Inorganic halide perovskite materials and solar cells*, **APL Materials**, **7(12)**, 2019, p. 120702. DOI: 10.1063/1.5117306.

[97] Zenghua W., Junjie L., Xiaojia Z., Wen-Hua Z., Yong Q., *Solution Processed Nb2O5 Electrodes for High Efficient Ultraviolet Light Stable Planar Perovskite Solar Cells*, **ACS Sustainable Chemistry & Engineering, 7(7)**, 2019, pp. 7421-7429. DOI: 10.1021/acssuschemeng.9b00991.

[98] Li, H., Li, F., Shen, Z., Han, S., Chen, J., & Dong, C. et al. *Photoferroelectric perovskite solar cells: Principles, advances and insights*, **Nano Today**, **37**, 2021, p. 101062. DOI: 10.1016/j.nantod.2020.101062.

[99] Kermani, H., Fallah, H., Hajimahmoodzadeh, M., & Tabatabaei, S., *Very low resistance ZnS/Ag/ZnS/Ag/ZnS nano-multilayer anode for organic light emitting diodes applications,* **Applied Optics**, **52(4)**, 2013, p. 780. DOI: 10.1364/ao.52.000780.

[100] Özer, N., Chen, D., Lampert, C., *Preparation and properties of spin-coated Nb2O5 films by the sol-gel process for electrochromic applications*, **Thin Solid Films**, **277(1-2)**, 1996, pp. 162-168. DOI: 10.1016/0040-6090(95)08011-2.

[101] Hsieh, T., Wei, T., Wu, K., Ikegami, M., Miyasaka, T., *Efficient perovskite solar cells fabricated using an aqueous lead nitrate precursor*, **Chemical Communications, 51(68),** 2015, pp. 13294-13297. DOI: 10.1039/c5cc05298j.

[102] Wei, J., Guo, F., Wang, X., Xu, K., Lei, M., Liang, Y., Zhao, Y., Xu, D., *SnO2 -in-Polymer Matrix for High-Efficiency Perovskite Solar Cells with Improved Reproducibility and Stability*, **Advanced materials (Deerfield Beach, Fla.), 30(52),** 2018, p. e1805153. DOI:10.1002/adma.201805153.

[103] Djurišić, A., He, Y., Ng, A., *Visible-light photocatalysts: Prospects and challenges*, **APL Materials, 8(3),** 2020, p. 030903. DOI: 10.1063/1.5140497.

[104] Ashok, B., Kewei, W., Arif, S., Erkki, A., Omar, F.M., Tom, W., *Perovskite Oxide SrTiO3 as an Efficient Electron Transporter for Hybrid Perovskite Solar Cells*, **The Journal of Physical Chemistry C, 118(49),** 2014, p. 28494-28501. DOI: 10.1021/jp509753p.

[105] Aydin, E., Liu, J., Ugur, E., Azmi, R., Harrison, G., Hou, Y. et al., *Ligand-bridged charge extraction and enhanced quantum efficiency enable efficient n–i–p perovskite/silicon tandem solar cells*, **Energy &Amp; Environmental Science, 14(8),** 2021, pp. 4377-4390. DOI: 10.1039/d1ee01206a.

[106] Yixin, Z., Alexandre, M.N., Kai, Z., *Solid-State Mesostructured Perovskite CH3NH3PbI3mSolar Cells: Charge Transport, Recombination, and Diffusion Length*, **The Journal of Physical Chemistry Letters, 5(3),** 2014, pp. 490-494. DOI: 10.1021/jz500003v.

[107] Yang, G., Chen, C., Yao, F., Chen, Z., Zhang, Q., Zheng, X., Ma, J., Lei, H., Qin, P., Xiong, L., Ke, W., Li, G., Yan, Y., Fang, G., *Effective Carrier-Concentration Tuning of SnO2 Quantum Dot Electron-Selective Layers for High-Performance Planar Perovskite Solar Cells*, **Advanced materials (Deerfield Beach, Fla.), 30(14),** 2018, p. e1706023. DOI:10.1002/adma.201706023.

[108] Thomas, A., *High-Efficiency Dye-Sensitized Solar Cells: A Comprehensive Review*, **Computational aAnd Experimental Research in Materials and Renewable Energy, 5(1),** 2022, pp. 1-29. DOI:10.19184/cerimre.v5i1.31475.

[109] Wang, C., Tang, Y., Hu, Y., Huang, L., Fu, J., Jin, J. et al., *Graphene/SrTiO3nanocomposites used as an effective electron-transporting layer for high-performance perovskite solar cells*, **RSC Advances, 5(64),** 2015, pp. 52041-52047. DOI:10.1039/c5ra09001f.

[110] Son. D.-Y., Bae K.-H., Kim H.-S., Park N.-G., *Effects of Seed Layer on Growth of ZnO Nanorod and Performance of Perovskite Solar Cell*, **The Journal of Physical Chemistry C, 119(19),** 2015, pp. 10321-10328. DOI: 10.1021/acs.jpcc.5b03276.

[111] Wang, K., Wang, X., Li, Z., Yang, B., Ling, M., Gao, X. et al., *Designing 3d dual transition metal electrocatalysts for oxygen evolution reaction in alkaline electrolyte: Beyond oxides*, **Nano Energy, 77,** 2020, p. 105162. DOI: 10.1016/j.nanoen.2020.105162.

[112] Wu, W., Chen, D., Huang, F., Cheng, Y., Caruso, R., *Sub-100 °C solution processed amorphous titania nanowire thin films for high-performance perovskite solar cells*, **Journal Of Power Sources, 329,** 2016, pp. 17-22. DOI: 10.1016/j.jpowsour.2016.08.061.

[113] Papageorgiou, D., Kinloch, I., Young, R. *Mechanical properties of graphene and graphene-based nanocomposites*, **Progress in Materials Science, 90,** 2017, 75-127. DOI: 10.1016/j.pmatsci.2017.07.004.

[114] Singh, R., Parashar, M., *Origin of Hysteresis in Perovskite Solar Cells. Soft-Matter Thin Film Solar Cells*, **AIP Publishing (online), Melville, New York,** 2020, pp.1-42. DOI: 10.1063/9780735422414_001.

[115] Roose, B., Pathak, S., Steiner, U., *Doping of TiO2for sensitized solar cells,* **Chemical Society Reviews, 44(22),** 2015, pp. 8326-8349. DOI: 10.1039/c5cs00352k.

[116] Gao, XX, Ge, QQ, Xue, DJ, Ding, J, Ma, JY, Chen, YX, Zhang, B, Feng, Y, Wan, LJ, Hu, JS, *Tuning the Fermi-level of TiO2 mesoporous layer by lanthanum doping towards efficient perovskite solar cells,* **Nanoscale**, **8**, 2016, pp. 16881–16885. DOI:10.1039/C6NR0 5917A.

[117] Zhang, B, Song, Z, Jin, J, Bi, W, Li, H, Chen, C, Dai, Q, Xu, L, Song H, *Efficient rare earth co-doped TiO2 electron transport layer for high-performance perovskite solar cells*, **J Colloid Interface Sci**, **553,** 2019, pp. 14–21. DOI:10.1016/j.jcis.2019.06.003.

[118] Zhu, Y., Zhu, Y., Deng, K., Sun, H., Gu, B., Lu, H., Cao, F., Xiong, J., Li, L., *TiO2 phase junction electron transport layer boosts efficiency of planar perovskite solar cells*, **Adv Sci., 5(3),** 2018, p.1700614. DOI:10.1002/advs.20170 0614.

[119] Manseki, K., Ikeya, T., Tamura, A., Ban, T., Sugiura, T., Yoshida, T., *Mg-doped TiO2 nanorods improving open-circuit voltages of ammonium lead halide perovskite solar cells*, **RSC Adv, 4(19),** 2014, pp. 9652–9655. DOI:10.1039/C3RA4 7870J.

[120] Cai, M., Wu, Y., Chen, H., Yang, X., Qiang, Y., Han, L., *Cost-performance analysis of perovskite solar modules*, **Adv Sci, 4,** 2017, p. 1600269. DOI:10.1002/advs.20160 0269.

[121] Tseng, Z.L., Chiang, C.H., Chang, S.H., Wu, C.G., *Surface engineering of ZnO electron transporting layer via Al doping for high efficiency planar perovskite solar cells*, **Nano Energy, 28,** 2016, 311–318. DOI:10.1016/j.nanoe n.2016.08.035.

[122] Zheng, Y., Zhao, E., Meng, F., Lai, X., Dong, X., Wu, J., Tao, X., *Iodine-doped ZnO nanopillar arrays for perovskite solar cells with high efficiency up to 18.24%*, **Journal Of Materials Chemistry A, 5(24),** 2017, pp. 12416-12425. DOI: 10.1039/c7ta03150e.

[123] Mahmud, M.A., Elumalai, N.K., Upama, M.B., Wang, D., Chan, K.H., Wright, M., Xu, C., Haque, F., Uddin, A., *Low Temperature Processed ZnO Thin Film as Electron Transport Layer for Efficient Perovskite Solar Cells*, **Solar Energy Materials and Solar Cells, 159,** 2017, 251-264. DOI:10.1016/j.solmat.2016.09.014.

[124] Azmi, R., Oh, S.-H., Jang S.-Y., *High-Efficiency Colloidal Quantum Dot Photovoltaic Devices Using Chemically Modified Heterojunctions,* **ACS Energy Letters, 1(1),** 2016, pp.100-106. DOI: 10.1021/acsenergylett.6b00070.

[125] Mahmood, K., Swain, B., Jung, H., *Controlling the surface nanostructure of ZnO and Al-doped ZnO thin films using electrostatic spraying for their application in 12% efficient perovskite solar cells*, **Nanoscale, 6(15),** 2014 p. 9127. DOI: 10.1039/c4nr02065k.

[126] Shin, S., Suk, J., Kang, B., Yin, W., Lee, S., Noh, J. et al., *Energy-level engineering of the electron transporting layer for improving open-circuit voltage in dye and perovskite-based solar cells*, **Energy &Amp; Environmental Science, 12(3),** 2019, pp. 958-964. DOI:10.1039/c8ee03672a.

[127] Shang, H., Zuo, Z., Zheng, H., Li, K., Tu, Z., Yi, Y. et al., *N-doped graphdiyne for high-performance electrochemical electrodes*, **Nano Energy, 44,** 2018, pp. 144-154. DOI:10.1016/j.nanoen.2017.11.072.

[128] Sans, J.A., Sánchez-Royo, J.F., Segura, A., Tobias, G., Canadell, E., *Chemical effects on the optical band-gap of heavily doped ZnO: M III (M = Al, Ga, In): an investigation by means of photoelectron spectroscopy, optical measurements under pressure, and band structure calculations,* **Phys Rev B, 79(19),** 2009, p. 195105. DOI:10.1103/PhysR evB.79.195105.

[129] Mahmood, K., Khalid, A., Ahmad, S.W., Mehran, M.T., *Indiumdoped ZnO mesoporous nanofibers as efficient electron transporting materials for perovskite solar cells*, **Surf Coat Technol, 352,** 2018, pp. 231–237. DOI:10.1016/j.surfc oat.2018.08.039.

[130] Nakazaki, J., Segawa, H., *Evolution of organometal halide solar cells*m **Journal Of Photochemistry And Photobiology C: Photochemistry Reviews, 35,** 2018, pp. 74-107. DOI:10.1016/j.jphotochemrev.2018.02.002.

[131] Shi, Z., Jayatissa, A.H., P*erovskites-Based Solar Cells: A Review of Recent Progress, Materials and Processing Methods*, **Materials (Basel, Switzerland), 11(5),** 2018, 729. DOI:10.3390/ma11050729.

[132] Dong, Q., Shi, Y., Zhang, C., Wu, Y., Wang, L., *Energetically favored formation of SnO2 nanocrystals as electron transfer layer in perovskite solar cells with high efficiency exceeding 19%*, **Nano Energy, 40,** 2017, pp. 336–344. DOI:10.1016/j.nanoen.2017.08.041.

[133] Elham, H. A., Ahmad, K., Matthew, T. M., Ludmilla, S., Taha, A., Silver-Hamill, T.-C., Jiyoun, S., Jingshan, L., Shaik, M.Z., Wolfgang, R. T., Tomas, E., Michael, G., Anders, H., Juan-Pablo, C.-B., *Low-Temperature Nb-Doped SnO2 Electron-Selective Contact Yields over 20% Efficiency in Planar Perovskite Solar Cells*, **ACS Energy Letters, 3(4)**, 2018, pp. 773-778. DOI:10.1021/acsenergylett.8b00055.

[134] Kai, W., Yantao, S., Qingshun, D., Yu, L., Shufeng, W., Xufeng, Y., Mengyao, W., Tingli, M., *Low-Temperature and Solution-Processed Amorphous WOX as Electron-Selective Layer for Perovskite Solar Cells*, **The Journal of Physical Chemistry Letters, 6 (5),** 2015, pp. 755-759. DOI: 10.1021/acs.jpclett.5b00010.

[135] Santaya, M., Troiani, H. E., Caneiro, A., Mogni, L.V., *Ternary Ni–Co–Fe Exsolved Nanoparticles/Perovskite System for Energy Applications: Nanostructure Characterization and Electrochemical Activity*, **ACS Applied Energy Materials, 3(10),** 2020, pp. 9528-9533. DOI: 10.1021/acsaem.0c01997.

[136] Chen, R., Cao, J., Duan, Y., Hui, Y., Chuong, T. T., Ou, D., Han, F., Cheng, F., Huang, X., Wu, B., Zheng, N., *High-Efficiency, Hysteresis-Less, UV-Stable Perovskite Solar Cells with Cascade ZnO-ZnS Electron Transport Layer*, **Journal of the American Chemical Society, 141(1),** 2019, pp. 541–547. DOI:10.1021/jacs.8b11001.

[137] Cao, T., Chen, K., Chen, Q., Zhou, Y., Chen, N., Li, Y., *Fullerene Derivative-Modified SnO2 Electron Transport Layer for Highly Efficient Perovskite Solar Cells with Efficiency over 21%*, **ACS Applied Materials & Interfaces, 11(37),** 2019**,** pp. 33825-33834. DOI: 10.1021/acsami.9b09238.

[138] Liao, JF., Li, WG., Rao, HS. et al., *Inorganic cesium lead halide CsPbX3 nanowires for long-term stable solar cells*, **Sci. China Mater, 60**, pp. 285–294. DOI:10.1007/s40843-017-9014-9.

[139] Chen, J., Huang, X., Sun, B., Wang, Y., Zhu, Y., Jiang, P., *Vertically Aligned and Interconnected Boron Nitride Nanosheets for Advanced Flexible Nanocomposite Thermal Interface Materials*, **ACS Applied Materials & Interfaces, 9(36)**, 2017, pp. 30909-30917. DOI: 10.1021/acsami.7b08061.

[140] Wojciechowski, K., Stranks, S.D., Abate, A., Sadoughi, G., Sadhanala, A., Kopidakis, N., Rumbles, G., Li, C.-Z., Friend, R.H., Jen, A.K.-Y., Snaith, H.J., *Heterojunction Modification for Highly Efficient Organic–Inorganic Perovskite Solar Cells*, **ACS Nano, 8(12),** 2014, pp. 12701-12709. DOI: 10.1021/nn505723h.

[141] Zuo, L., Chen, Q., De Marco, N., Hsieh, Y. T., Chen, H., Sun, P., Chang, S. Y., Zhao, H., Dong, S., Yang, Y., *Tailoring the Interfacial Chemical Interaction for High-Efficiency Perovskite Solar Cells*, **Nano letters, 17(1),** 2017, pp. 269–275. DOI:10.1021/acs.nanolett.6b04015.

[142] Han, G., Chung, H., Kim, B., Kim, D., Lee, J., Swain, B. et al., *Retarding charge recombination in perovskite solar cells using ultrathin MgO-coated TiO2 nanoparticulate films*, **Journal Of Materials Chemistry A, 3(17),** 2015, pp. 9160-9164. DOI:10.1039/c4ta03684k.

[143] Chen, Q., De Marco, N., Yang, Y., Song, T., Chen, C., Zhao, H. et al., *Under the spotlight: The organic–inorganic hybrid halide perovskite for optoelectronic applications*, **Nano Today, 10(3),** 2015, pp. 355-396. DOI: 10.1016/j.nantod.2015.04.009.

[144] Agubra, V., Zuniga, L., Flores, D., Villareal, J., Alcoutlabi, M., *Composite Nanofibers as Advanced Materials for Li-ion, Li-O2 and Li-S Batteries*, **Electrochimica Acta, 192,** 2016, pp. 529-550. DOI: 10.1016/j.electacta.2016.02.012.

[145] Kumar, R., *NiCo2O4 Nano-/Microstructures as High-Performance Biosensors: A Review*, **Nano-micro letters, 12(1)**, 2020, p. 122. DOI:10.1007/s40820-020-00462-w.

[146] Liu, D., Yang, C., Bates, M., Lunt, R. R., *Room Temperature Processing of Inorganic Perovskite Films to Enable Flexible Solar Cells*, **iScience, 6,** 2018, pp. 272–279. DOI:10.1016/j.isci.2018.08.005.

[147] Zhou, H., Chen, Q., Li, G., Luo, S., Song, T. B., Duan, H. S., Hong, Z., You, J., Liu, Y., Yang, Y., *Photovoltaics. Interface engineering of highly efficient perovskite solar cells*, **Science (New York, N.Y.), 345(6196),** 2014, pp. 542–546. DOI:10.1126/science.1254050.

[148] Mamun, A., Ava, T., Abdel-Fattah, T., Jeong, H., Jeong, M., Han, S. et al., *Effect of hot-casted NiO hole transport layer on the performance of perovskite solar cells*, **Solar Energy, 188,** 2019, pp. 609-618. DOI: 10.1016/j.solener.2019.06.040.

[149] Liu, Z., Chen, Q., Hong, Z., Zhou, H., Xu, X., De Marco, N., Sun, P., Zhao, Z., Cheng, Y.-B., Yang, Y., *Low-Temperature TiOx Compact Layer for Planar Heterojunction Perovskite Solar Cells*, **ACS Applied Materials & Interfaces, 8(17),** 2016, pp. 11076-11083. DOI: 10.1021/acsami.5b12123.

[150] Mali, S., Shim, C., Kim, H., Patil, P., Hong, C., *In situ processed gold nanoparticle-embedded TiO2nanofibers enabling plasmonic perovskite solar cells to exceed 14% conversion efficiency*, **Nanoscale, 8(5),** 2016, pp. 2664-2677. DOI: 10.1039/c5nr07395b.

[151] Zhou, Y., Yang, S., Yin, X., Han, J., Tai, M., Zhao, X. et al., *Enhancing electron transport via graphene quantum dot/SnO2 composites for efficient and durable flexible perovskite photovoltaics*, **Journal Of Materials Chemistry A, 7(4),** 2019, pp. 1878-1888. DOI:10.1039/c8ta10168j.

[152] Wang, K., Shi, Y., Gao, L., Chi, R., Shi, K., Guo, B. et al., *W(Nb)O x -based efficient flexible perovskite solar cells: From material optimization to working principle*, **Nano Energy, 31,** 2017, pp. 424-431. DOI: 10.1016/j.nanoen.2016.11.054.

[153] Yang, D., Yang, R., Wang, K., Wu, C., Zhu, X., Feng, J., Ren, X., Fang, G., Priya, S., Liu, S. F., *High efficiency planar-type perovskite solar cells with negligible hysteresis using EDTA-complexed SnO2*, **Nature communications, 9(1),** 2018, p. 3239. DOI:10.1038/s41467-018-05760-x.

[154] Lu, Z., Pan, X., Ma, Y., Li, Y., Zheng, L., Zhang, D. et al., *Plasmonic-enhanced perovskite solar cells using alloy popcorn nanoparticles*, **RSC Advances, 5(15),** 2015, pp. 11175-11179. DOI: 10.1039/c4ra16385k.

[155] Liu, Y., Zhang, Q., Xu, M., Yuan, H., Chen, Y., & Zhang, J. et al. *Novel and efficient synthesis of Ag-ZnO nanoparticles for the sunlight-induced photocatalytic degradation*. **Applied Surface Science**, **476**, 2019, pp. 632-640. DOI: 10.1016/j.apsusc.2019.01.137.

[156] Lin, S., Xia, P., Wu, S., Zhang, W., Hu, Y., & Liu, B. et al. *Passivating the interface between halide perovskite and SnO2 by capsaicin to accelerate charge transfer and retard recombination*, **Applied Physics Letters**, **120(10)**, 2022, p. 103503. doi: 10.1063/5.0082785

[157] Yella, A., Heiniger, L. P., Gao, P., Nazeeruddin, M. K., & Grätzel, M., *Nanocrystalline rutile electron extraction layer enables low-temperature solution processed perovskite photovoltaics with 13.7% efficiency*. **Nano letters**, **14(5)**, 2014, p. 2591–2596. DOI: 10.1021/nl500399m

[158] Jiang, P., Acharya, D., Volonakis, G., Zacharias, M., Kepenekian, M., & Pedesseau, L. et al. *Pb-free halide perovskites for solar cells, light-emitting diodes, and photocatalysts*, **APL Materials**, **10(6)**, 2022, p. 060902. DOI: 10.1063/5.0095515

[159] Ouyang, S., Zhang, J., Yu, F., & Qin, L. *A vibration energy harvester based on Ca3TaGa3Si2O14 piezoelectric crystal for high temperature applications*, **Applied Physics Letters**, **115(25)**, 2019, p. 253901. DOI: 10.1063/1.5127658

[160] Fang, R., Wu, S., Chen, W., Liu, Z., Zhang, S., Chen, R., Yue, Y., Deng, L., Cheng, Y. B., Han, L., & Chen, W., *[6,6]-Phenyl-C61-Butyric Acid Methyl Ester/Cerium Oxide Bilayer Structure as Efficient and Stable Electron Transport Layer for Inverted Perovskite Solar Cells*, 2018, **ACS nano, 12(3),** pp. 2403–2414. DOI: 10.1021/acsnano.7b07754.

[161] Yuji O., Yoshikazu S., *Mesoporous BaTiO3/TiO2 Double Layer for Electron Transport in Perovskite Solar Cells*, **The Journal of Physical Chemistry C, 120 (26)**, 2016, pp. 13995-14000, DOI: 10.1021/acs.jpcc.6b04642.

[162] Thakur, U., Kisslinger, R., Shankar, K. *One-Dimensional Electron Transport Layers for Perovskite Solar Cells*, **Nanomaterials**, **7(5)**, 2017, p. 95. DOI: 10.3390/nano7050095.

[163] Chandrasekhar, P., Komarala, V. *Graphene/ZnO nanocomposite as an electron transport layer for perovskite solar cells; the effect of graphene concentration on photovoltaic performance*, **RSC Advances, 7(46)**, 2017, pp. 28610-28615. DOI: 10.1039/c7ra02036h.

[164] Mohamad Noh M.F., Arzaee, N., Mumthas, I., Mohamed, N., MN, E., Safaei J., Yusoff, A., Nazeeruddin, M., Mat T., Mohd A., *High-Humidity Processed Perovskite Solar Cells*, **Journal of Materials Chemistry A. 8**, 2020, DOI: 10.1039/D0TA01178A.

[165] Shahiduzzaman, M., Fukaya, S., Muslih, E. Y., Wang, L., Nakano, M., Akhtaruzzaman, M., Karakawa, M., Takahashi, K., Nunzi, J. M., & Taima, T., *Metal Oxide Compact Electron Transport Layer Modification for Efficient and Stable Perovskite Solar Cells*. **Materials (Basel, Switzerland)**, **13(9)**, 2020, 2207. DOI: 10.3390/ma13092207.

[166] Fang, R., & Lin, Y. *Enhancement of perovskite photoluminescence characterizations by using lithography-free metal nanostructures*, **AIP Advances**, **10(6)**, 2020 p. 065328. DOI: 10.1063/5.0011590.

[167] You, Y., Tian, W., Min, L., Cao, F., Deng, K., Li, L., *TiO2/WO3 Bilayer as Electron Transport Layer for Efficient Planar Perovskite Solar Cell with Efficiency Exceeding 20%*, **Adv. Mater. Interfaces, 7**, 2020, p. 1901406. DOI: 10.1002/admi.201901406.

[168] Li, Y., Xie, H., Lim, E. L., Hagfeldt, A., Bi, D., *Recent Progress of Critical Interface Engineering for Highly Efficient and Stable Perovskite Solar Cells*, **Adv. Energy Mater.**, **12**, 2022, p. 2102730. DOI: 10.1002/aenm.202102730.

[169] Rasouli, S., Rezaei, N., Hamedi, H., Zendehboudi, S., Duan, X., *Superhydrophobic and superoleophilic membranes for oil-water separation application: A comprehensive review*, **Materials Amp; Design**, **204**, 2021, p. 109599. DOI: 10.1016/j.matdes.2021.109599.

[170] Weijun K., Constantinos C. S., Jenna L.L., Michael R. W., Yanfa Y., Guojia F., and Mercouri G. K., *TiO2–ZnS Cascade Electron Transport Layer for Efficient Formamidinium Tin Iodide Perovskite Solar Cells*, **Journal of the American Chemical Society, 138 (45)**, 2016, pp. 14998-15003. DOI: 10.1021/jacs.6b08790.

[171] Chavan, R., Yadav, P., Tavakoli, M., Prochowicz, D., Nimbalkar, A., & Bhoite, S. et al. *Double layer mesoscopic electron contact for efficient perovskite solar cells*, **Sustainable Energy &Amp; Fuels**, **4(2)**, 2020, pp. 843-851. DOI: 10.1039/c9se01051c.

[172] Mahmoudi, T., Wang, Y., Hahn, Y.-B., *SrTiO3/Al2O3-Graphene Electron Transport Layer for Highly Stable and Efficient Composites-Based Perovskite Solar Cells with 20.6% Efficiency*, **Adv. Energy Mater. 10**, 2020, 1903369. DOI: 10.1002/aenm.201903369.

[173] Z. Chen, F. Mo, T. Wang, Q. Yang, Z. Huang, D. Wang, G. Liang, A. Chen, Q. Li, Y. Guo, X. Li, J. Fan and C. Zhi, *A semi-conductive organic cathode material enabled by extended conjugation for rechargeable aqueous zinc batteries*, **Energy Environ. Sci., 14,** 2021, p. 2441.

[174] Hengjie Liu, Qun He, Hongliang Jiang, Yunxiang Lin, Youkui Zhang, Muhammad Habib, Shuangming Chen, and Li, *Electronic Structure Reconfiguration toward Pyrite NiS2via Engineered Heteroatom Defect Boosting Overall Water Splitting*, **Song ACS Nano 2017 11 (11),** 11574-11583 DOI: 10.1021/acsnano.7b06501.

[175] Xing, Z., Li, SH., Xu, PY. et al. *Crystallographic Understanding of Photoelectric Properties for C60 Derivatives Applicable as Electron Transporting Materials in Perovskite Solar Cells*, **Chem. Res. Chin. Univ. 38,** 2022, pp. 75–81 DOI: 10.1007/s40242-021-1264-6.

[176] Shahiduzzaman, M., Fukaya, S., Muslih, E., Wang, L., Nakano, M., & Akhtaruzzaman, M. et al. *Metal Oxide Compact Electron Transport Layer Modification for Efficient and Stable Perovskite Solar Cells* **Materials**, **13(9)**, 2020, p. 2207. DOI: 10.3390/ma13092207

[177] Xu, X., Zhang, H., Shi, J., Dong, J., Luo, Y., Li, D., & Meng, Q. *Highly efficient planar perovskite solar cells with a TiO2/ZnO electron transport bilayer*, **Journal Of Materials Chemistry A**, **3(38),** 2015, pp. 19288-19293. DOI: 10.1039/c5ta04239a.

[178] Chih-Yu C., Kuan-Ting L., Wen-Kuan H., Hao-Yi S., and Yu-Chia C., *High-Performance, Air-Stable, Low-Temperature Processed Semitransparent Perovskite Solar Cells Enabled by Atomic Layer Deposition*, **Chemistry of Materials**, **27(14)**, 2015, pp. 5122-5130. DOI: 10.1021/acs.chemmater.5b01933.

[179] Groner M. D., Fabreguette F. H., Elam J. W., and George S. M., *Low-Temperature Al2O3 Atomic Layer Deposition*, **Chemistry of Materials**, **16(4),** 2004, pp. 639-645. DOI: 10.1021/cm0304546

[180] Godin, R., Ma, X., González-Carrero, S., Du, T., Li, X., Lin, C.-T., McLachlan, M. A., Galian, R. E., Pérez-Prieto, J., Durrant, J. R., *Tuning Charge Carrier Dynamics and Surface Passivation in Organolead Halide Perovskites with Capping Ligands and Metal Oxide Interfaces*, **Advanced Optical Materials**, **6**, 2018, p. 1701203. DOI: 10.1002/adom.201701203

[181] Ono, Luis & Leyden, Matthew & Wang, Shenghao & Qi, Yabing, *Organometal Halide Perovskite Thin Films and Solar Cells by Vapor Deposition*, **J. Mater. Chem. A., 4**, 2015. DOI: 10.1039/C5TA08963H.

[182] Niu, G., Li, W., Meng, F., Wang, L., Dong, H., & Qiu, Y. *Study on the stability of CH3NH3PbI3films and the effect of post-modification by aluminum oxide in all-solid-state hybrid solar cells*, **J. Mater. Chem. A, 2(3)**, 2014, pp. 705-710. doi: 10.1039/c3ta13606j

[183] Xu, Y., Li, Z., He, C., Li, J., Ouyang, T., & Zhang, C. et al. *Intrinsic piezoelectricity of monolayer group IV–V MX2: SiP2, SiAs2, GeP2, and GeAs2*, **Applied Physics Letters**, **116(2)**, 2020, p. 023103. DOI: 10.1063/1.5135950

[184] Leijtens, T., Eperon, G. E., Pathak, S., Abate, A., Lee, M. M., & Snaith, H. J. *Overcoming ultraviolet light instability of sensitized TiO_2 with meso-superstructured organometal tri-halide perovskite solar cells*, **Nature communications**, **4**, 2013, p. 2885. DOI: 10.1038/ncomms3885

[185] Zhao, X., Shen, H., Zhang, Y., Li, X., Zhao, X., Tai, M., Li, J., Li, J., Li, X., & Lin, H. *Aluminum-Doped Zinc Oxide as Highly Stable Electron Collection Layer for Perovskite Solar Cells*, **ACS applied materials & interfaces**, **8(12)**, 2016, pp. 7826–7833. DOI: 10.1021/acsami.6b00520

[186] He, J., Zhang, R., Shao, M., Zhao, X., Miao, M., Chen, J., Liu, J., Zhang, X., Zhang, X., Jin, Y., Wang, Y., Zhang, S., Zhu, L., Jacob, A., Jia, R., You, X., Li, X., Li, C., Zhou, Y., Yang, Y., Li,

Z. *Efficacy and safety of low-dose IL-2 in the treatment of systemic lupus erythematosus: a randomised, double-blind, placebo-controlled trial*, **Annals of the rheumatic diseases**, **79(1)**, 2020, pp. 141–149. DOI: 10.1136/annrheumdis-2019-215396

[187] Tavakoli, M., Tavakoli, R., Yadav, P., & Kong, J. *A graphene/ZnO electron transfer layer together with perovskite passivation enables highly efficient and stable perovskite solar cells*, **Journal Of Materials Chemistry A**, **7(2)**, 2019, pp. 679-686. DOI: 10.1039/c8ta10857a.

[188] Wang, K., Lou, Y., Li, M., Li, X., Femi, I., & Yang, Y. et al. *Induced charge transfer bridge by non-fullerene surface treatment for high-performance perovskite solar cells*, **Applied Physics Letters**, **115(18)**, 2019, p. 183503. DOI: 10.1063/1.5124539.

[189] Wu, X., Yu, H., & Cao, J. *Unraveling the origin of resistive switching behavior in organolead halide perovskite based memory devices*, **AIP Advances**, **10(8)**, 2020, p. 085202. DOI: 10.1063/1.5130914.

[190] Ruiqian M., Xiaoxia F., Yiwei Y., Xudong L., Jing C., and Yu Tang, *Cerium-Oxide-Modified Anodes for Efficient and UV-Stable ZnO-Based Perovskite Solar Cells*, **ACS Applied Materials & Interfaces**, **11 (14)**, 2019, pp. 13273-13278. DOI: 10.1021/acsami.9b01587

[191] Gill Sang Han, Jio Kim, Seunghwan Bae, Sehoon Han, Yong Joo Kim, Oh Yeong Gong, Phillip Lee, Min Jae Ko, and Hyun Suk Jung, *Spin-Coating Process for 10 cm × 10 cm Perovskite Solar Modules Enabled by Self-Assembly of SnO2 Nanocolloids*, **ACS Energy Letters, 4 (8)**, 2019, pp. 1845-1851. DOI: 10.1021/acsenergylett.9b00953.

[192] Hwang, K., Jung, Y. S., Heo, Y. J., Scholes, F. H., Watkins, S. E., Subbiah, J., Jones, D. J., Kim, D. Y., & Vak, D. *Toward large scale roll-to-roll production of fully printed perovskite solar cells*. **Advanced materials (Deerfield Beach, Fla.), 27(7)**, 2015, pp. 1241–1247. DOI: 10.1002/adma.201404598.

[193] Zou, Y., Yu, W., Tang, Z., Li, X., Guo, H., & Liu, G. et al. *Improving interfacial charge transfer by multi-functional additive for high-performance carbon-based perovskite solar cells*, **Applied Physics Letters**, **119(15)**, 2021, p. 151104. DOI: 10.1063/5.0061869.

[194] Xin L., Yequan X., Qiugui Z., Jiexuan J., and Yanbo L., *Large-Area Organic-Free Perovskite Solar Cells with High Thermal Stability*, **The Journal of Physical Chemistry Letters, 10 (20)**, 2019, pp. 6382-6388. DOI: 10.1021/acs.jpclett.9b02644.

[195] Tang, Q., Zhou, Z. and Chen, Z., *Innovation and discovery of graphene-like materials via density-functional theory computations*. **WIREs Comput Mol Sci, 5**, 2015, pp. 360-379. DOI: 10.1002/wcms.1224.

[196] Manser, J., & Kamat, P. *Band filling with free charge carriers in organometal halide perovskites*, **Nature Photonics**, **8(9)**, 2014, pp. 737-743. DOI: 10.1038/nphoton.2014.171.

Received: September 15, 2022
Accepted: October 18, 2022